SKRIFTER NR. 188

BERT RUDELS

On the mass balance of the Polar Ocean, with special emphasis on the Fram Strait

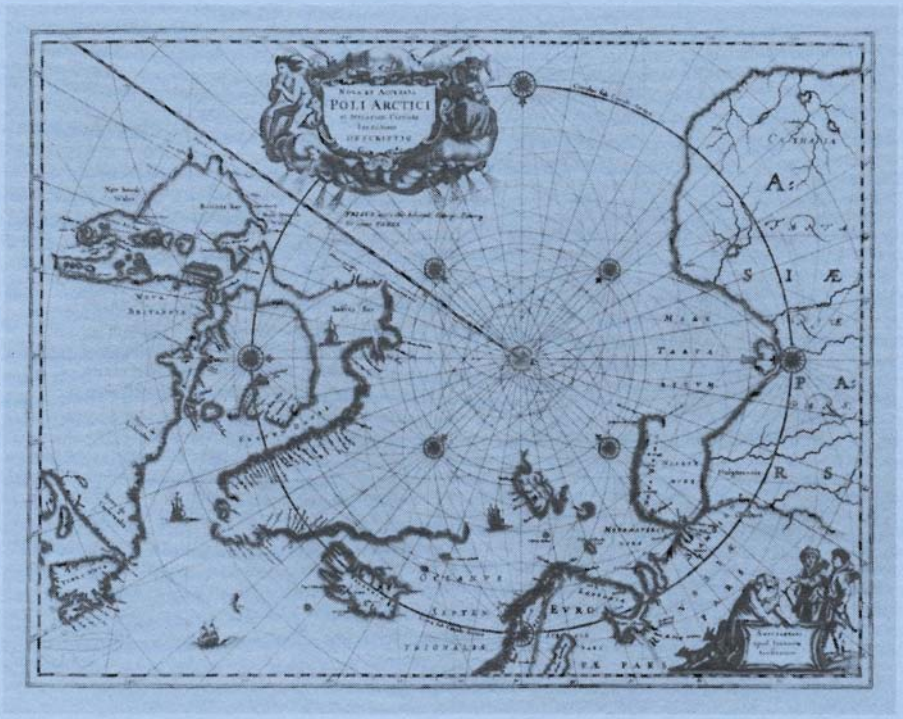

NORSK POLARINSTITUTT
OSLO 1987

SKRIFTER NR. 188

BERT RUDELS

On the mass balance of the Polar Ocean, with special emphasis on the Fram Strait

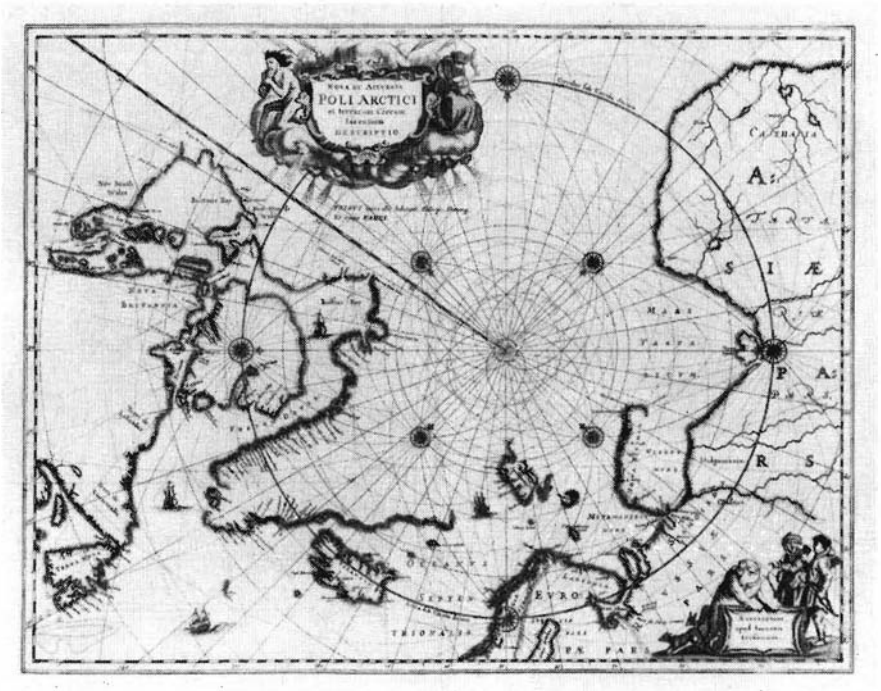

NORSK POLARINSTITUTT
OSLO 1987

Contents

ISBN 82-90307-46-2
Printed April 1987

On the mass balance of the Polar Ocean, with special emphasis on the Fram Strait

BERT RUDELS

Rudels, B. 1987: On the mass balance of the Polar Ocean, with special emphasis on the Fram Strait. *Norsk Polarinstitutt Skrifter 188:* 1–53.

The transports of mass, heat, and salt through the four main passages to the Polar Ocean are estimated. The exchanges through the Fram Strait are found from the geostrophic velocity field computed on two sections across the passage, obtained by HMS 'Ymer' in August 1980 and by M/S 'Lance' in August 1983, where the level of no motion has been determined by a variational approach, subject to some general continuity requirements.

The lighter, fresher surface water present in summer is likely to affect and distort the results. The transport estimates are thus uncertain, but the obtained values indicate smaller exchanges than are usually assumed.

A substantial part of the Atlantic water in the West Spitsbergen Current is found to recirculate in the northern vicinity of the strait, and what is perhaps the largest contribution of Atlantic water to the Polar Ocean may enter over the Barents Sea.

Bert Rudels, Norsk Polarinstitutt, Rolfstangveien 12, 1330 Oslo Lufthavn, Norway.

1. Introduction

The exchanges between the North Atlantic and the Polar Ocean through the Fram Strait are computed from two CTD sections, one obtained from HMS 'Ymer' in 1980, and the other from M/S 'Lance' in 1983.

Geostrophically balanced flow is assumed, and a variational approach is used to determine the unknown barotropic velocity field. The total kinetic energy

$$2^{-1} \int_A \varrho v^2 \, dx dz$$

of the flow through the entire cross section is minimized, subject to some general constraints. To formulate these constraints a closer look at the exchanges through the other passages and at water mass properties in the different basins is necessary.

The geography and hydrography of the Polar Ocean are briefly reviewed in section 2. The freshwater balance is discussed in section 3. Transports through the Bering Strait, the Barents Sea, and the Arctic Archipelago are considered in sections 4–6.

In section 7 the hydrography in the Fram Strait is presented in part 1, and the baroclinic velocities are computed in part 2. The variational method is discussed in part 3 and applied to different constraints in parts 4 and 5.

The transports are summarized and compared with other etstimates in section 8, and finally in section 9 a few speculative comments on the nature of the circulation in the Polar Ocean are given.

2. The Polar Ocean

By the Polar Ocean we understand the area (Vowinckel & Orvig 1970) bounded to the south by the American continent, the Arctic Archipelago, Greenland, the Fram Strait, Svalbard, and the line connecting the northeast of Svalbard with the northern cape of Novaja Zemlja. The boundary then continues north-south along Novaja Zemlja to the Eurasian continent,

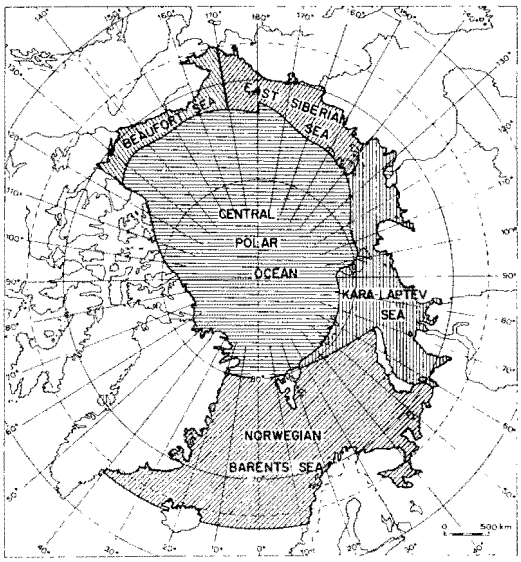

Fig. 1. Map of the Polar Ocean. (From Vowinchel & Orvig 1970.)

which together with the Bering Strait close the area (Fig. 1). The Polar Ocean then consists of the central Polar basin, about 4000 m deep, which is divided by the 1600 m deep Lomonosov ridge into the Amerasian and Eurasian basins, and of the marginal seas, which with their extensive shelves occupy 1/3 of the total area of $9 \cdot 10^{12}$ m^2. The straits in the Arctic Archipelago, Baffin Bay, the Greenland/Norwegian Seas, and the Barents Sea are excluded by this definition. The Polar Ocean is the largest mediterranean sea in the world, and its communication with the rest of the world oceans takes place through four restricted passages: The Arctic Archipelago, the Fram Strait, the Barents Sea, and the Bering Strait.

The oceanography of the Polar Ocean is affected by the opposing effects of freshwater discharge from the rivers and heat loss at the sea surface. In spite of excessive cooling and the removal of freshwater by ice formation the positive buoyancy contribution of the river discharge dominates and creates a stratification, which inhibits vertical mixing in most of the water column. Not only water advected from the Atlantic and the Pacific but also waters deriving from the shelf areas are therefore clearly distinguished in the interior of the Polar Ocean.

2.1. Water masses

Four distinct water masses may be recognized. These water masses, however, exhibit large spatial and perhaps temporal variations, reflecting their different mixing histories. In presenting these water masses we shall mainly follow the review by Coachman & Aagaard (1974).

The polar mixed layer is a 50 m deep, low saline (about 32) layer with the temperature near the freezing point. This layer is homogenized locally during the winter by haline convection, possibly aided by keel stirring. In the summer a shallow (10–20 m) fresher surface layer is formed by the ice melt. The presence of ice, however, forces the temperature to remain close to the freezing point. The properties of the polar mixed layer vary over the basin. It is deeper ($\sim$ 100 m) and more saline ($\sim$ 33) close to the Fram Strait, while its salinity may be less than 30 in the Beaufort Sea.

Beneath the homogeneous polar mixed layer a 100–150 m thick *pycnocline* is encountered. The increased density is due to a strong halocline, while the temperature may remain at the freezing point down to 100 m. This feature excludes the possibility of forming the pycnocline through mixing between the polar mixed layer and the underlying warm Atlantic water (Coachman & Barnes 1961). A more likely source is the large shelf areas, where cold dense water can be formed in the winter through brine rejection (Coachman & Barnes 1961; Aagaard et al. 1981). This water is then advected into the interior of the basin at its density level. This view is supported by the higher salinities observed in the pycnocline off the shelves close to the principal salt source – the Atlantic (Aagaard et al. 1981).

The horizontal variations in temperature observed in the pycnocline are due to two effects: The water close to the shelves is at freezing point, and the freezing point temperature varies with the salinities of the waters on the different shelves. In the interior of the basin, the temperature increases from the interaction, perhaps by double-diffusive convection, with the underlying warmer layer.

Near to the Bering Strait the presence of Pacific water affects the pycnocline. It becomes thicker ($\sim$ 300 m) and contains both a temperature maximum (T $\sim$ –1.0°C, S $\sim$ 32.5) at 75 m and a temperature minimum (T $\sim$ –1.5°C, S $\sim$ 33.5) at 150 m due to the inflow of summer- and winter water, respectively, through the Bering Strait (Coachman & Barnes 1963). The temperature minimum may, however, also be formed during the winter on the Chukchi shelves (Jones & Anderson, pers. comm.).

Over the entire Polar Ocean *Atlantic water*, commonly defined as water with temperature greater than 0°C, is encountered. The maximum temperature is above 2°C close to the Fram Strait, while in the Beaufort Sea and northeast of Greenland it is below 0.5°C. As it enters north of Svalbard the Atlantic water constitutes a salinity maximum (S $\sim$ 35.0) in the water column. This maximum is rapidly removed and the salinity attains a rather constant value of 34.9. The thickness of the Atlantic layer is about 600 m.

The *deep water* has an almost constant salinity of about 34.94, while the temperature decreases with depth and reaches –0.9°C at the bottom of the Eurasian basin. In the Amerasian basin the temperature is higher (–0.5°C) and constant below 1600 m, which reflects the presence of the Lomonosov ridge. The difference in temperature between the two basins supports the view advanced by Nansen that the deep water derives from the Atlantic. Whether a possible inflow of deep water from the Greenland/Norwegian Seas constitutes the sole source of the polar deep water, or if additional contributions come from the Barents Sea and perhaps from the shelves inside the Polar Ocean, is an open and challenging question (Nansen 1906; Swift et al. 1983; Aagaard et al. 1985; Rudels 1986b).

2.2. Water movements

The circulation in the upper layers of the Polar Ocean, as revealed by the ice drift, is anticyclonal and dominated by the strong transpolar drift, which passes approximately over the North Pole from Siberia towards the Fram Strait. The dynamic topography of the surface conforms well with this picture and suggests that the anticyclonal windfield over the Polar Ocean creates a 'high' in the Beaufort Sea, which, in addition to the wind, drives the upper layers and the ice towards the Fram Strait.

By contrast the flow of the pycnocline and the Atlantic and deep water is cyclonal. This can be inferred from the temperature of the Atlantic water, as it moves along the Eurasian slope. The temperature decreases from the Fram Strait towards the east, reflecting the movement of the water (Coachman & Barnes 1962).

The inflow from the Pacific may, to a crude approximation, be considered as short-circuited between the Bering Strait and the Arctic Archipelago.

3. Freshwater discharge and ice-export

The main freshwater source for the Polar Ocean is the river discharge, most of which derives from the Siberian rivers Ob, Yenisei, and Lena, and the Mackenzie river in Alaska. The discharge exhibits large seasonal variations with practically no flow during the winter and a sharp peak in May–June. The yearly variations are also large and may be 10–15% of the mean annual discharge. The most cited figure for the contribution from the rivers is $0.10 \cdot 10^6$ m^{3}s^{-1} (SCOR WG–58 1979), which will be adopted here.

The amount of precipitation and evaporation in the Polar Ocean is poorly known. Mosby (1962) suggests a precipitation of $0.03 \cdot 10^6$ m^{3}s^{-1} and an evaporation of $0.02 \cdot 10^6$ m^{3}s^{-1}. We have chosen the value $0.02 \cdot 10^6$ m^{3}s^{-1} for net precipitation, expecting it to be higher than Mosby's value.

This gives a total freshwater contribution of $0.12 \cdot 10^6$ m^{3}s^{-1}. It is the total amount which is of interest, and the actual partition between river discharge and precipitation is of less importance.

Because of the ice formation which occurs in the Polar Ocean, a large fraction of freshwater is removed from the water column and exported as ice. The size of the ice-export is difficult to estimate. The areal extent of the ice cover, which passes through the Fram Strait, by far the most important exit for the Polar ice, can be assessed from satellite images. The width of the ice stream varies between 250 and 440 km. The average drift speed is found to be about 9.5 cm s^{-1}. The observations of the drift are dependent upon the identification of individual floes, and since little cloud-cover occurs mainly in connection with northerly winds, this may be an overestimate (Vinje 1982). With this value the annual area export ranges between 0.75 and $1.32 \cdot 10^{12}$ m^2. However, later observations indicate values between 0.6 and $0.9 \cdot 10^{12}$ m^2 (Vinje 1983).

The largest uncertainty in the estimates of ice-export is due to our ignorance of the ice thicknesses. Traditionally an ice thickness of 3 m has been assumed (Zubov 1945), but recent measurements in the Fram Strait suggest that 4 to 5 m may be more appropriate.

We have assumed that $0.08 \cdot 10^6$ m^{3}s^{-1} of freshwater is exported as ice. This corresponds to an annual area export of $0.84 \cdot 10^{12}$ m^2 with an ice thickness of 3 m. The salinity of the ice is taken to be 3, and its density 1000 kg m^{-3}.

The existence of a low saline top layer in the Arctic strongly suggests that the freshwater exported as ice is less than the river discharge. However, freshwater deriving from the Bering Strait inflow could also supply the needed water. In addition, ice formation on the shelves may fractionate the water column by creating water denser than the surface layer (Aagaard et al. 1981). This sinks deeper into the water column and enforces the impression of a positive net buoyancy contribution and an increased (as compared to the inflow) stability in the Polar Ocean.

The adopted ice export is small (Vinje & Finnekåsa 1986; Östlund & Hut 1984), but for our purpose it is the amount of freshwater in the water column which is of importance. Its value $0.04 \cdot 10^6$ m^{3}s^{-1} is hardly more than a guess (see discussion in section 8).

4. The Bering Strait

The communication between the Polar and the Pacific oceans takes place through the narrow (80 km) and shallow ($\sim$ 50 m) Bering Strait. The principal direction of the flow is from the Pacific into the Polar Ocean.

The dominating driving force is the higher sea level in the Pacific as compared to the Arctic. The slope in sea level creates a meridional pressure gradient, which, balanced mainly by friction, drives the water through the strait. It has been suggested that the

difference in sea level is caused by the lower salinity in the Pacific as compared to the Atlantic water column (Stigebrandt 1981a, 1984).

The transports show large variations and are clearly influenced by local meteorological conditions (Coachman et al. 1975). Recently reported current-measurements (Coachman & Aagaard 1981) also indicate a strong seasonal cycle of the fluxes. In the summer the northward transport average is $1.2 \cdot 10^9$ kg s^{-1}, while in the winter it is as low as $0.4 \cdot 10^9$ kg s^{-1}. Variations have been mentioned earlier, especially in the Russian literature (see Coachman & Aagaard 1974). The cause of the fluctuations seems to be a more frequent occurrence of strong events of southward flow during the winter months (Coachman & Aagaard 1981).

The salinity in the Bering Sea in the summer is 32.4 (Aagaard & Greisman 1975; Coachman & Aagaard 1974), while in the winter it becomes substantially higher; 33.2 might be a reasonable value (cf. Coachman & Aagaard 1974). Assuming that the ice produced in the Bering Sea is transported with the water into the Polar Ocean, the salinity of the combined flow of ice and water will remain 32.4 even in the winter. However, the observations by Schumacher et al. (1983) indicate that the ice transport is more influenced by the winds than the water movements. It is then conceivable that ice is driven southwards in the winter due to the prevailing northerly winds, while the bulk of the run-off is carried north with the currents during the summer. While it is, therefore, quite likely that there exists a yearly salinity variation in the combined inflow, it will be ignored henceforth.

The average transport through the Bering Strait is $0.8 \cdot 10^9$ kg s^{-1} with the salinity 32.4. It may be of some interest, especially with respect to the heat budget, to look at the two seasons separately. The transport of summer water is $0.6 \cdot 10^9$ kg s^{-1} with $S = 32.4$ and $T = 5.0°C$ (Coachman & Aagaard 1974), and the amount of winter water is $0.2 \cdot 10^9$ kg s^{-1} with $S = 33.2$ and $T = -1.8°C$ (freezing point).

The ice transport may be estimated from $M_w S_w = (M_w + M_i)S_s$ where S_s, S_w are the summer and winter salinities, M_w is the wintertime water transport, and M_i is the ice transport. Introducing the values proposed above we get $M_i = 0.005 \cdot 10^9$ kg s^{-1}. This is a small amount in the mass budget, but may be of some importance in the heat budget, where we obtain a heat flux of $0.4 \cdot 10^9$ kcal s^{-1}.

This is close to the value found by Aagaard & Greisman (1975) by another method. The water column entering the Polar Ocean has a depth of 50 m, and the estimated ice-transport corresponds to an ice thickness of 1.2 m if the ice moves with the water.

The contributions from the Bering Strait and from the other passages are collected in Table 1.

5. The Barents Sea

Aagaard & Greisman (1975) accepted Mosby's (1938) estimate of inflow from the Polar Ocean to the Barents Sea between Svalbard and Frans Josef Land ($0.1 \cdot 10^9$ kg s^{-1}, $S = 34.9$, $\theta = 2.7°C$) based upon data from the 'Quest' cruise in 1931. However, recent current measurements in the channel between Storøya and Nordaustlandet indicate a weak but persistent flow to the north (Aagaard et al. 1983). Also in the main channel between Victoria Island and Frans Josef Land, where Mosby's observations were made, the presence of colder, fresher water close to the bottom on the eastern side suggests a flow into the Polar Ocean. There is also a sharp temperature and salinity gradient between the Atlantic water found north and south of the sill between Storbanken and Edgeøya (Pfirman 1984). The lower salinities found to the north as well as the existing current measurements thus confine this northern inflow to the northern part of the Barents Sea. A conceivable flow pattern would be that the Atlantic water from the Polar Ocean 'hangs' on the banks around

Table 1. Contributions to the mass, heat and salt budgets of the Polar Ocean, excluding the Fram Strait transports.

Passage	Mass transport 10^9 kg/s	Temp. °C	Heat transport* 10^9 kcal/s	Sal.	Salt transport 10^6 kg/s
Bering Strait					
Summer Water	0.6	5	3.0	32.4	19.44
Winter Water	0.2	-1.8	-0.36	32.4	6.48
Ice	0.005	-1.8	-0.40		
Arctic Archipelago					
Surface Water	-0.7	-1.0	0.7	32.9	-23.03
Deep Exchange	-0.3	-0.5	0.15	34.3	-10.29
Barents Sea					
Coastal Water	0.8	-1.8	-1.44	34.85	27.88
Atlantic Water	0.4	1.0	0.4	35.05	14.02
Run off	0.10	5	0.5	–	–
Net. precip.	0.02	–	–	–	–
Ice export	0.08	-1.8	6.54	3.0	0.24
Total transport	1.04		8.3		34.74

* Transport relative to 0°C.

Kvitøya and Victoria Island, entering through Frans Victoria Renna and returning to the Polar Ocean between Storøya and Kvitøya. The assumed northerly flow along the eastern slope of Frans Victoria Renna would then probably have a southern source.

Aagaard & Greisman (1975) estimate the flow from the Barents Sea into the Kara Sea between Frans Josef Land and Novaja Zemlja to be $0.7 \cdot 10^9$ kg s^{-1} with $\theta = 0.9$°C and S = 34.7, making a net inflow from the Atlantic to the Polar Ocean across the Barents Sea of $0.6 \cdot 10^9$ kg s^{-1}. Since this value is based upon requirements of mass continuity for the entire Polar Ocean, we choose to form an independent estimate of the conditions encountered in the Barents Sea.

In the Barents Sea the boundary between Atlantic and Polar influences is clearly indicated at the sea surface by the extension of the ice cover. To the north sea-ice is present during most of the year. The surface temperatures are, therefore, close to the freezing point. The southern part is normally ice free in the summer, but during the winter an ice cover develops in the eastern parts, and the ice limit roughly coincides with the extent of the shallow shelf areas west of Novaja Zemlja. The ice cover is also influenced by the prevailing winds, and open water may appear close to the coast of Novaja Zemlja (Vinje priv.comm.).

The inflow of water of Atlantic origin consists of two different water masses. Close to the coast the continuation of the Norwegian coastal current enters into the Barents Sea. Its water has an average salinity of 34.85, and it can be followed as a relatively fresh, warm tongue as it moves into the Barents Sea. It flows along the coast and has lost most of its heat when it reaches Novaja Zemlja (Nansen 1906). The coastal water overrides underlying Atlantic water, and its largest depth is about 200 m close to the coast and decreases towards the north.

While the coastal water enters the Barents Sea as a wedge attached to the coast, the

deeper lying Atlantic water follows the depth contours northward along the Norwegian continental slope and does not turn eastward until it reaches the Bear Island Channel. The main part of this warm, $\theta = 3.5°C$, and saline, $S = 35.05$, Atlantic water seems to be prevented, perhaps by the topography, from continuing east and north of the central banks in the Barents Sea, beyond which the Atlantic water is substantially cooler and fresher, indicating a northern origin (see above). Most of the Atlantic water entering from the south thus returns, after losing some of its heat to the atmosphere, to the Atlantic in the Bear Island Current.

An alternative explanation of the absence of the warm, salty Atlantic water in the northern and eastern parts of the Barents Sea could be that it is transformed as it passes over the sills between Storbanken and Sentralbanken and between Edgeøya and Storbanken. Such transformations can result from mixing, perhaps isopycnally, with comparably dense cold water formed through brine rejection over shallow areas, or by local vertical mixing, if the surface layer by freezing should attain a high enough salinity to allow convection into the Atlantic water.

The northern part of the Barents Sea is dominated by a westward motion of polar surface water, which enters the area both south and north of Frans Josef Land. Some of this water continues north of Svalbard towards the west, but the main part passes south of Svalbard to follow the West Spitsbergen Current back to the Polar Ocean (Tancjura 1959).

The energy loss q through the sea surface in the southern Barents Sea is high, averaging 75 W m^{-2} over the year (Bunker priv.comm.). The required heat is mainly supplied by the cooling of inflowing water from the west. This value will be used to estimate the inflow over the Barents Sea. The areal extent A of the southern part is taken to be $0.6 \cdot 10^{12}$ m^2, and the total heat loss is $qA = Q = 45 \cdot 10^{12}$ W, or $10.75 \cdot 10^9$ kcal s^{-1}. The surface temperature of the coastal water as it enters the Barents Sea varies between 8–12°C throughout the year (Climatological Atlas). Between 100–200 m the temperature is about 4°C, and if we take this to be constant over the year we would get an average temperature of $\theta_C = 7°C$ for the coastal water ($S_C = 34.85\%$). For the Atlantic water the corresponding values are $\theta_A = 3.5°C$, $S_A = 35.05$ (Nansen 1906; Blindheim & Loeng 1981). The densities of the waters become $\rho_C = 1.0275$ and $\rho_A = 1.0279$ g cm^{-3} respectively. The amount of coastal water entering the Barents Sea can be found from Werenskjold's formula (Defant 1961). It states that if the lighter surface water is confined to the coast and the denser motionless underlying water reaches the surface, then a knowledge of the density of the two layers and the depth of the upper layer at the coast is sufficient to determine the transport in the upper layer.

$$M_C = \frac{g(\rho_A - \rho_C)H^2}{2f\rho} \rightarrow M_C = 0.8 \cdot 10^9 \text{ kg s}^{-1}$$

This water flows over the Barents Sea and presumably enters the Polar ocean over the Kara Sea passing between Novaja Zemlja and Frans Josef Land. Some part may also reach the Polar Ocean west of Frans Josef Land. Timofeyev suggests that about $0.6 - 1.0 \cdot 10^9$ kg s^{-1} enters the Kara Sea between Frans Josef Land and Novaja Zemlja (Coachman & Aagaard 1974; Fletcher 1965). The coastal water will lose its heat on its way across the Barents Sea and the heat flux becomes

$$Q_c = \Delta\theta M_c = 7.2 \cdot 10^9 \text{ Kcal s}^{-1}$$

with $\Delta\theta = (\theta_c - 0) = 9$ °C

if the temperature θ of the coastal water is at the freezing point when it reaches Novaja Zemlja. This seems reasonable, since ice is formed each winter in the eastern Barents Sea,

but requires that the incoming water does not pass too quickly across the Barents Sea. A crude estimate of the residence time of the coastal water in the Barents Sea is therefore needed. The width $B = 0.2 \cdot 10^6$ m of the tongue of coastal water does not change significantly as it flows towards the east (Nansen 1906). The time T, needed for a water particle to move the distance L from the Atlantic to the eastern Barents Sea, is then approximately

$$T = LHB\,M\bar{C}^1,\ H = 100\text{ m and } L = 10^6\text{ m}$$

which gives $T = 0.25 \cdot 10^9$ s $\sim$ 1 year. A water particle which passes over the Barents Sea must, therefore, pass through one winter cooling during which it loses heat.

Now $Q_C\,Q^{-1} = 2/3$ and an additional heat source is needed to obtain a heat balance. The only remaining source is the cooling of Atlantic water either directly in the southwestern part of the sea, or in the deep in the other areas. Substantial brine rejection may in the latter case be needed to increase the density of the surface water sufficiently to drive a convection down into the Atlantic water and make the water column overturn and transport heat from the Atlantic water to the atmosphere. Moreover, water with salinity greater than 35 and at the freezing point is only rarely observed in the Barents Sea. We therefore assume that the Atlantic water loses a fraction of its heat mainly due to cooling in the Hopen deep and over Sentralbanken. The horizontal charts given by Nansen (1906) and the observed difference in θ–S characteristics indicate great changes in the Atlantic water mass between the Hopen deep and the depressions further to the east and north. This supports the view that the principal heat loss occurs in the western Barents Sea. Most of the cooled Atlantic water probably returns to the west in the Bear Island Channel, but some may pass over the sills into the northern and eastern part of the Barents Sea, and continue into the Polar Ocean (Tancjura 1959). We tentatively assume that 1/3 of the transformed AW enters the Polar Ocean.

The Fugløy-Bjørnøya section shown by Blindheim & Loeng (1981) gives the temperature of the inflowing water. It represents observations taken during the autumn, and we may assume that the mean temperature of the Atlantic water entering over the year is lower, and put it to 3.5°C. The cold water found at the bottom and on the northern slope of the section represents the Atlantic return flow. If the temperature of the Atlantic water is lowered from 3.5°C to 1.0°C, the mass $M_a = (Q\text{–}Q_c) \cdot \Delta\theta_a^{-1}$ must be cooled to obtain heat balance in the Barents Sea. M_a then becomes $1.44 \cdot 10^9$ kg s^{-1}, of which $0.4 \cdot 10^9$ kg s^{-1} enters the Polar Ocean and the rest returns to the Atlantic.

In the heat budget we have ignored the contribution from ice formation, assuming that the ice formed in the southern Barents Sea also melts there. Tritium and O^{18}/O^{16} measurements indicate that no river discharge is present in the Barents Sea (Östlund priv. comm.). However, the water, which discharges into the Polar Ocean, has on average a slightly lower salinity, 34.7 (Aagaard & Greisman 1975), when it enters the Barents Sea. The dilution of the water of Atlantic origin must be the result of the melting of sea-ice drifting south from the Polar Ocean, or, less likely, by a southward flow of polar water with a large component of melt water. To assess the largest possible effect on the estimate of the inflow over the Barents Sea, the lowering of the salinity is assumed to be the result solely of ice melt.

The net ice melt necessary to achieve a change in salinity from 34.92 to 34.7 is $7.5 \cdot 10^6$ kg s^{-1} and would require additional heat import by the Atlantic waters. The heat loss which corresponds to this melting of ice is $0.6 \cdot 10^9$ kcal s^{-1}. This is roughly 6% of the heat loss through the sea surface. This contribution is ignored.

Due to irregular bottom topography of the Barents Sea the effects of winter cooling and

ice formation show large local variations. In the shallower areas the convection reaches to the bottom, and the entire water column will be at the freezing point with a gradually increasing salinity as the ice formation proceeds. In the deeper parts the surface water may not become dense enough to penetrate into the bottom water, which may have formed on a nearby shallow shelf or been advected from the Atlantic, but is only capable of homogenizing the upper layers. Finally, over areas of intermediate depths it would be possible to eventually overturn the entire water column but not to cool it to the freezing point.

All these different water masses will subsequently move along the channels and canyons into the Polar Ocean one water mass layered upon the other, giving the observed temperature and salinity profiles their extremely rugged appearances (Fig. 2). Because of the different densities of the water masses formed in the Barents Sea, we may expect them to enter the Polar Ocean not only in the pycnocline but also deeper down in the water column. These possiblilities were discussed at length already by Nansen (1906), and recently by Midttun (1985) and Swift et al. (1983).

With respect to the mass and salt balances, however, the transformation of the waters in the Barents Sea is of no importance. Freshwater, which leaves and returns to the Polar Ocean at the Barents Sea boundary, will not affect the estimated transports from the Atlantic to the Polar Ocean over the Barents Sea. We may again point out that the cooling of AW in the eastern part occurs through mixing of cold water either locally by penetrative

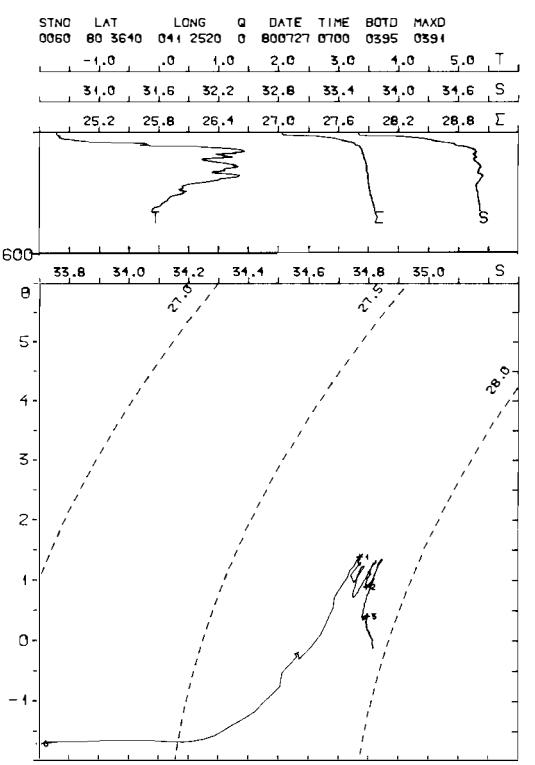

Fig. 2. θ, S and Σ profiles and θ–S diagram for stations taken in the Northern Barents Sea.

convection or isopycnally by advection from the shallow areas. In either case the high density has been reached through brine rejection, and the temperature change of the AW in this area is a reflection of ice production during the winter.

We conclude (Table 1) that in all $1.2 \cdot 10^9$ kg s^{-1} enters the Polar Ocean, and the total salt transport becomes $41.9 \cdot 10^6$ kg s^{-1}. The actual θ–S properties will, of course, be quite varied, and we expect the temperature to range from the freezing point to perhaps +1.0°C and the salinity from 34.4 to 35.0. The temperatures and salinities will be correlated with the preferred combinations cold-fresh and warm-salty.

The crude analysis above is not intended to be the final answer to the problem of the transports of the Barents Sea but should be looked upon as an estimate not contradicting the observations and useful as a first order approximation.

To get a feel for the uncertainties involved we may look at some possible sources of error. Bunker & Worthington (1977) give the heat exchange to 100 W m^{-2} instead of 75 W m^{-2}, which would increase the transports with about 20–25%. The estimate of the temperatures could well be off by 1–2°C, giving an uncertainty of 10%. In the dynamical approach the largest uncertainity is in the choice of upper layer depth, and here a discrepancy of 25 m will alter the estimate by 20%.

We have completely neglected the interaction between the water masses in the northern and the southern parts of the Barents Sea. Our main reason is the belief that most of this water will be carried back into the Polar Ocean. Some fraction does, however, pass south, as is seen by the fresh, cold southwestward flowing Bear Island Current. We have assumed that it carries $1 \cdot 10^9$ kg s^{-1} of mostly cooled and freshened Atlantic water back to the north Atlantic, ignoring any Polar contribution. Pfirman (1984) estimates the transport to $0.8 \cdot 10^9$ kg s^{-1}, but considers it to consist of $0.45 \cdot 10^9$ kg s^{-1} of water from the northern Barents Sea and perhaps ultimately from the Polar Ocean.

It should be noted that an outflow of fresher water from the northern Barents Sea to the Atlantic would result in a comparably higher salinity of the net inflow from the Atlantic to the Polar Ocean.

6. The Arctic Archipelago

A substantial part of the export of surface water takes place through the three channels Lancaster Sound, Jones Sound, and the Nares Strait in the Arctic Archipelago. These outflows all discharge into Baffin Bay to continue in the Baffin Current through the Davis Strait into the Labrador Sea. The flow is unidirectional, as through the Bering Strait, and the main driving mechanism is probably the lighter surface water found in the Beaufort Sea as compared to Baffin Bay. Muench (1971) states that the difference in steric heights between the two seas is about 0.3 db with respect to the 250 db level. The corresponding pressure gradient would be capable of driving the flow through the archipelago towards the Atlantic. However, in contrast to the conditions prevailing in the Bering Strait, these passages are deeper (200–250 m) and show substantial stratification. The dominating force balance is thus more likely to be geostrophy than a longitudinal pressure gradient opposed by friction.

Stigebrandt (1981b) has approximated the transports through the archipelago by a two-layer rotationally controlled flow and derived a transport of $2 \cdot 10^9$ kg s^{-1}. This is close to the figure most often found in the literature. However, the estimates show large variations and range from $0.7 \cdot 10^9$ kg s^{-1} to above $3 \cdot 10^9$ kg s^{-1}. Most of these values are obtained from dynamical calculations either in the individual channels, across Baffin Bay or in the Davis Strait. Only in a few instances have the computations been supplemented by direct current measurements (Sadler 1976). Reviews of the transport estimates and of the

hydrography of the archipelago and of Baffin Bay can be found in Bailey (1957), Coachman & Aagaard (1974), Collin & Dunbar (1963), Kiilerich (1939), and Muench (1971), and we shall here just present the main features of the hydrography in Baffin Bay.

Baffin Bay is a narrow elongated sea with the main entrance to the south at the Davis Strait (sill depth 640 m). The area is $0.4 \cdot 10^{12}$ m^2, and the maximum depth is more than 2400 m. The upper 200 metres are characterized by a cold core with a temperature of $-1.6°$ C and a salinity of 33.7 (Tchernia 1979). In the summer this core is capped by a fresher, warmer (2–5° C) surface layer, due to ice melt. The core is formed locally by ice formation during the winter.

Beneath the core a warm, 0.5–1.5° C, and saline, 34.5, 500–1000 m thick Atlantic layer is found. Part of this layer must enter from the south through the Davis Strait, but it is probably much diluted by water from the Polar Ocean. The deep water has almost constant θ–S characteristics with temperature –0.44° C and salinity 34.4.

The circulation is cyclonic. The West Greenland Current enters from the Labrador Sea and flows north along the Greenland coast. In the northern part it meets the Polar inflow, and the water returns to the Davis Strait in the Baffin Current to the west. It is likely that a substantial recirculation occurs at all levels north of the Davis Strait (Smith et al. 1937).

I have tried to obtain an independent estimate of transport (Rudels 1986a) using the approach of a rotationally constrained baroclinic flow (Stigebrandt 1981b). The effects both of the northern straits and of the Davis Strait have been taken into account, and a three reservoir system is considered, where all passages are assumed to transport at maximum capacity. Using the observed value of the salinity in the surface layer of Baffin Bay and the depth of the upper layer in the Beaufort Sea, the transport is obtained as a function of the salinity in the Beaufort Sea.

To decide what salinity value to use a second approach is adopted. The characteristic temperature and salinity of the cold core are established by transforming the inflowing water from the north running through the Davis Strait by convection driven by the ice formation during the winter.

It is then possible to form mass, heat, and salt balances for Baffin Bay, where the transports through the archipelago and in the West Greenland Current into Baffin Bay are functions of the amount of ice formed and of the salinity in the Beaufort Sea.

These two approaches are then combined to obtain a value acceptable to both methods. A transport of $0.7 \cdot 10^9$ kg s^{-1} with salinity 32.9 has thus been chosen (Rudels 1986a).

The results discussed so far only apply to the upper layers of Baffin Bay. The deeper parts of the water column, both the Atlantic layer and the deep water, contain a substantial and perhaps dominant part of water from the Arctic. It has been possible only to surmise this denser contribution to the outflow, and we tentatively suggest the value $0.3 \cdot 10^9$ kg s^{-1} with salinity 34.3 (Table 1). The total transport through the archipelago is hence rather small, and the suggested salinity is lower than the one found in most estimates (Stigebrandt 1981b; Aagaard & Greisman 1975).

7. The Fram Strait

The strait between Greenland and Svalbard – the Fram Strait – is by far the deepest passage (sill depth > 2500 m) connecting the Polar Ocean with the world oceans. Atlantic water as well as deep and bottom water may here communicate freely between the Polar Ocean and the North Atlantic. An inflow of deep water from the Greenland and Norwegian Seas may thus constitute a source for the deep and bottom waters in the Polar Ocean. While other sources are conceivable – inflow of cooled Atlantic water over the Barents Sea, cold saline water formed by brine rejection on the shelves – the sole exit for the Polar Ocean

deep water is through the Fram Strait. It is also the passage for the return flow of Atlantic water, and 90% of the ice export and (perhaps) the main outflow of Polar surface water pass here.

The principal water masses from the Polar Ocean and the Greenland and Norwegian Seas are brought into contact in the strait. The differences which exist between these water masses, reflect the processes active in the two regions. If we knew the nature and strength of the processes, the flow field and the exchanges through the Fram Strait could be determined. On the other hand, a knowledge of the transport may shed some light upon the mechanisms at work, primarily in the Polar Ocean.

Our present situation is that we have fragmentary knowledge at both ends, and we shall try to piece the information together to infer something both about the transports and about the mechanisms driving the Polar Ocean–Greenland/Norwegian Seas system. As will be seen below, such a view is admittedly optimistic. However, some information has been gained, and we shall present our approach in the subsequent parts.

The main arguments rest upon the assumption that the flow in the Fram Strait is geostrophic. Especially, we shall ignore the Ekman transports. In the summer the winds are variable, and the neglect is probably justified, but the northerly winds prevailing in the winter may result in a non-zero mean Ekman transport which will not be taken into account.

The geostrophic flow is driven by density differences which result from the thermodynamic processes active in the Polar Ocean and the Norwegian and Greenland Seas. The density distribution in the Fram Strait is furthermore influenced by the prevailing large scale wind fields and perhaps by topographically controlled boundary currents, which combine to create a density field and a sea level slope in the Fram Strait capable of maintaining a transport through the strait matching the transformations.

These transformations will impose constraints on the system, which can be used to determine the unknown level of no motion in the geostrophic field. Depending upon the generality of the applied constraints, information will also be gained about what processes are in agreement with these conditions. This can be used together with accepted knowledge of the processes active in the system to test the reliability of the solution. It should be kept in mind that the more detailed the required constraints, the less new information will be found about the active mechanisms.

The following discussion is based upon two hydrographic transects across the strait obtained in 1980 and 1983, and we shall search for the least energetic flow field capable of sustaining the necessary transports. This approach is applied in section 7.4 together with a requirement of mass and salt balance for the entire Polar Ocean.

As will be evident below, these constraints are too general and the obtained flow fields are rather unconvincing, especially with regard to the 1983 section. It is thus neither possible to deduce realistic transports nor infer anything about the mixing processes from these obvious requirements, and additional information is needed. In section 7.5 we therefore use the observed differences in salinity between the deeper layers in the Polar Ocean and in the Greenland/Norwegian Seas to form additional constraints. The resulting flow fields are then examined and compared with those found in section 7.4. The most reasonable velocity field will then be used to determine the transports, which are discussed in section 8.

7.1. Water masses in the Fram Strait

The hydrographic structure in the Fram Strait is displayed by the two sections. The first, taken from HMS 'Ymer' in August 1980, runs roughly along the sill at 79° N. The second,

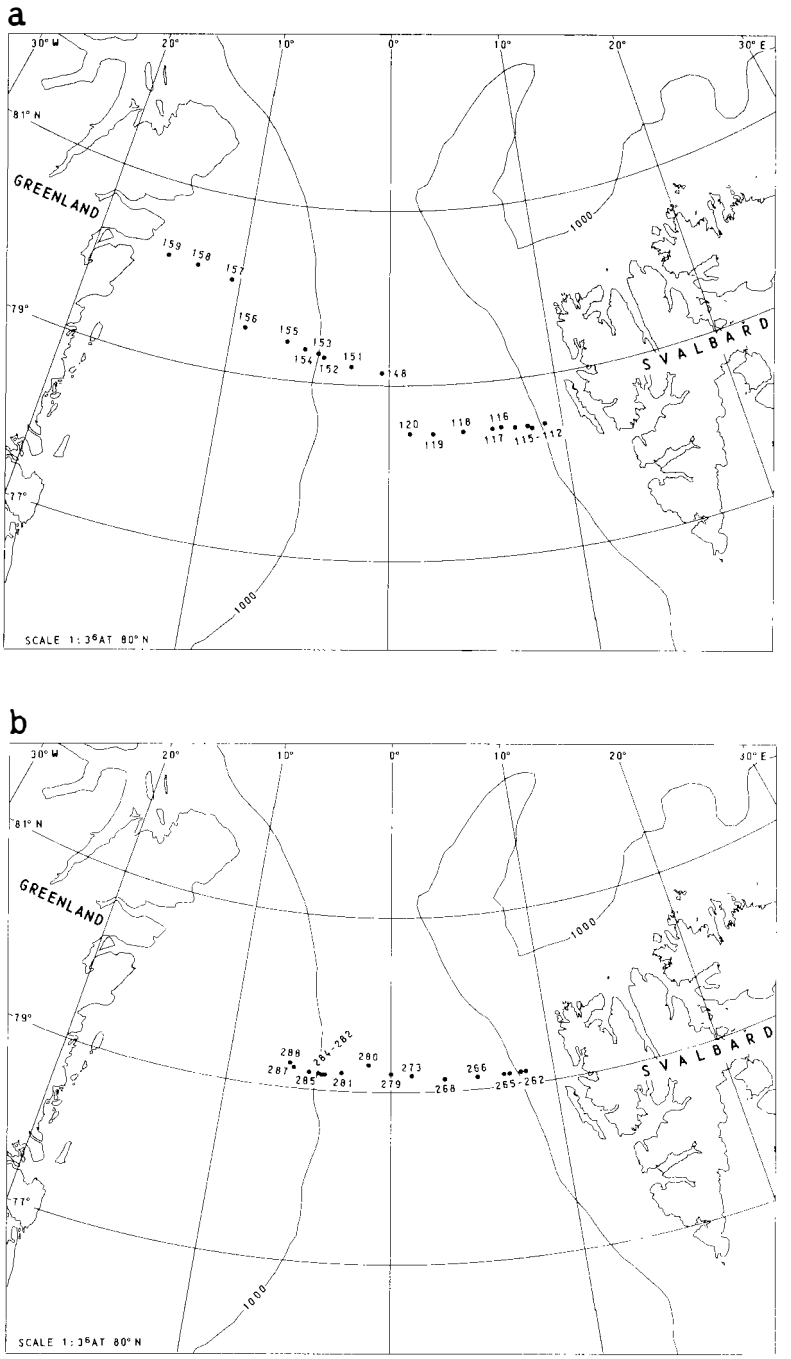

Fig. 3. Station chart in the Fram Strait.
a) 'Ymer' stations
b) 'Lance' staions

obtained from M/S 'Lance' in August 1983, lies somewhat further to the north at 79° 15′N (Fig. 3). This section passes over the Molloy Deep (depth 5540 m), and several stations do not reach to the bottom. Due to malfunctions in the conductivity cell some of the stations over the deeper part had to be excluded. A breakdown of the winch prevented us from

reaching our optimal depth (3400 m) on the neighbouring stations. It has, therefore, been necessary to perform horizontal interpolations in the deeper part of the second section. The 'Lance' section thus leaves much to be desired, but we consider it to be workable and close enough to the 'Ymer' section to allow for a comparison between the two years.

The sections have much in common (Figs. 4, 5). Most of the upper 500 m is warm, saline Atlantic water, which extends from Svalbard almost to the Greenland continental slope. This layer terminates suddenly to the west, where strong horizontal gradients in temperature and salinity are found. The salinity maximum disappears, and the maximum temperature decreases from above 2–3°C to less than 1°C. These changes are density compensating, and no corresponding large horizontal density gradient is observed.

While the structure of this Atlantic layer is similar in the two years, the temperatures and salinities are seen to be substantially higher in 1983. Whether such interannual variations are common, or if we in 1980 observed the passage of the 'mid-seventy salinity anomaly' (Dickson & Blindheim 1984) cannot be decided from the data at hand.

Above the Atlantic water low saline surface water is found over a large part of the passage. The thickness of this surface layer increases towards the west and completely dominates over the Greenland shelf.

In the deeper parts of the cross section the temperature decreases with depth, and the salinity drops below that of the Atlantic layer. There are, however, several extrema observed especially in the salinity distribution, which indicate strong interleaving and mixing between different water masses in the deep interior of the Fram Strait. A weak salinity minimum is found almost over the entire cross section. It is especially conspicuous in 1980, while it is weaker, colder, and found at lower levels in 1983.

Weak horizontal gradients are also observed in the deeper layers. The temperature and salinity increase towards the west, contrary to the situation in the upper layers.

To aid the identification and discussion of the different water masses in the strait, θ–S diagrams have been constructed for different areas as well as for the entire Fram Strait. In the 'Ymer' observations we shall regard stations 112–116 as belonging to the eastern, while stations 152–155 constitute the western part. The central area is divided into a central eastern (st. 117–120) and a central western (st. 148, 151) part. Stations 156–159 represent the shelf area. The corresponding stations for the 'Lance' section are: Eastern area 262–268, Central eastern 273, 276, Central western 279–281, and Western 282–288. No stations were obtained on the Greenland shelf in 1983.

We shall introduce six different water masses based upon θ–S characteristics. The partition is with some slight departures based upon the one introduced by Swift & Aagaard 1981. Water masses I: $\theta < 0$, $S < 34.7$, II: $0 < \theta$, $S < 34.5$, IIa: $0 < \theta < 1$, $34.5 < S < 34.7$, $1 < \theta$, $34.5 < S < 34.9$ comprise the low salinity waters. The cold deep waters $\theta < 0$, $S > 34.7$ are found in water mass III, while IV covers the range $0 < \theta < 1$, $34.7 < S$, and water masses V: $1 < \theta < 3$, $34.9 < S$ and VI: $3 < \theta$, $34.9 < S$ comprise the warm saline water masses. The division is indicated in the θ–S diagrams.

The most significant feature of the θ–S relations is perhaps that they are much tighter than our partition suggests. This gives us some hope that sensible information about mixing and water mass transformations can be inferred from the θ–S diagrams (Figs. 6, 7, 8).

The low saline cold polar surface water comprises water mass I, and it is found almost exclusively in the central western and western parts of the cross section. This water mass derives from the Polar Ocean, where it is formed from the dilution of AW with freshwater from precipitation and the river discharge and modified by cycles of ice formation and ice melt. It probably also contains Pacific water, which has entered the Polar Ocean through the Bering Strait. While water mass I thus represents the most marked polar feature of the cross sections, the main Atlantic influence is found in the warm saline water masses V and

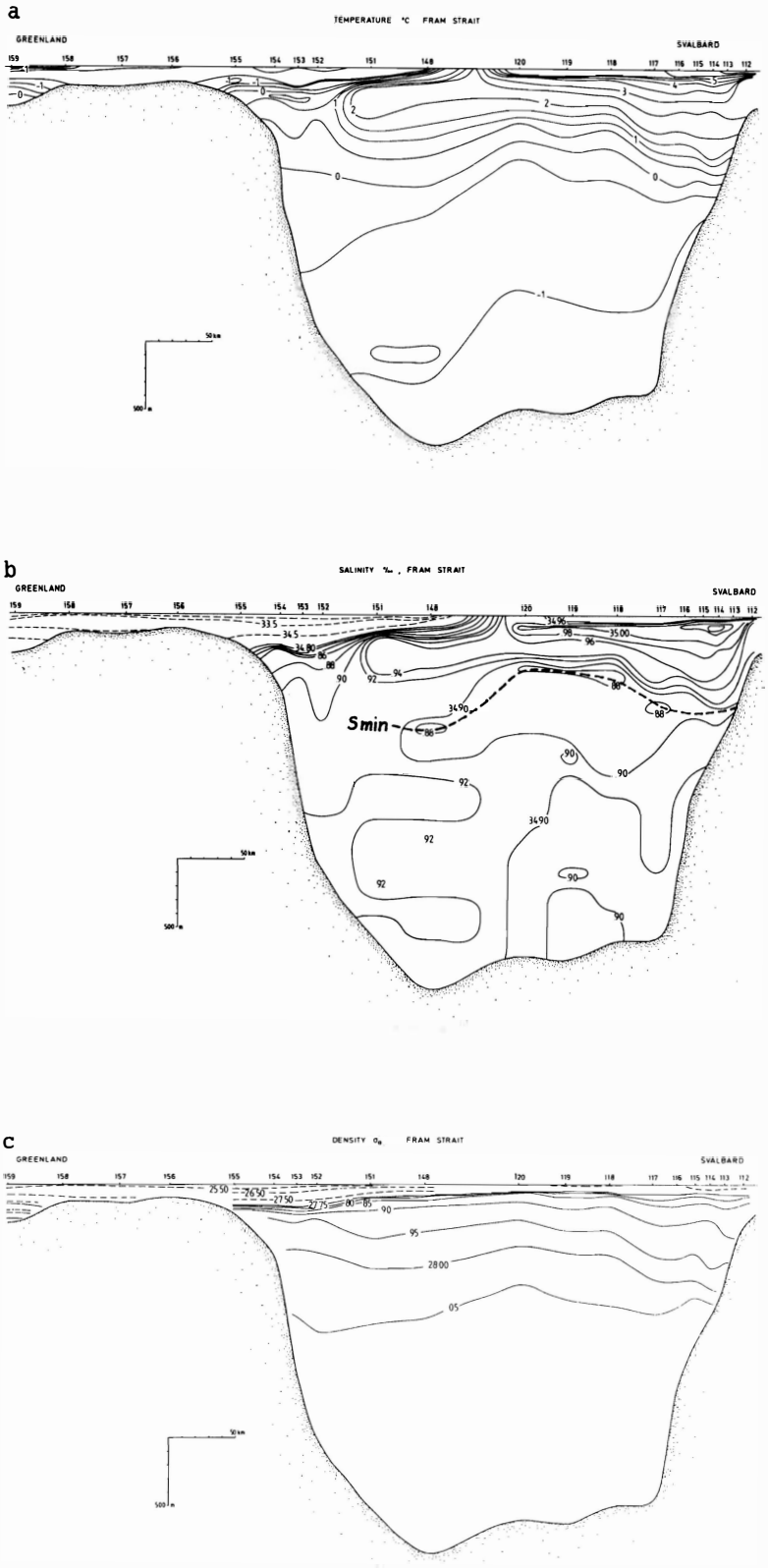

Fig. 4a–c. Sections of potential temperature, salinity and potential density: 'Ymer' section.

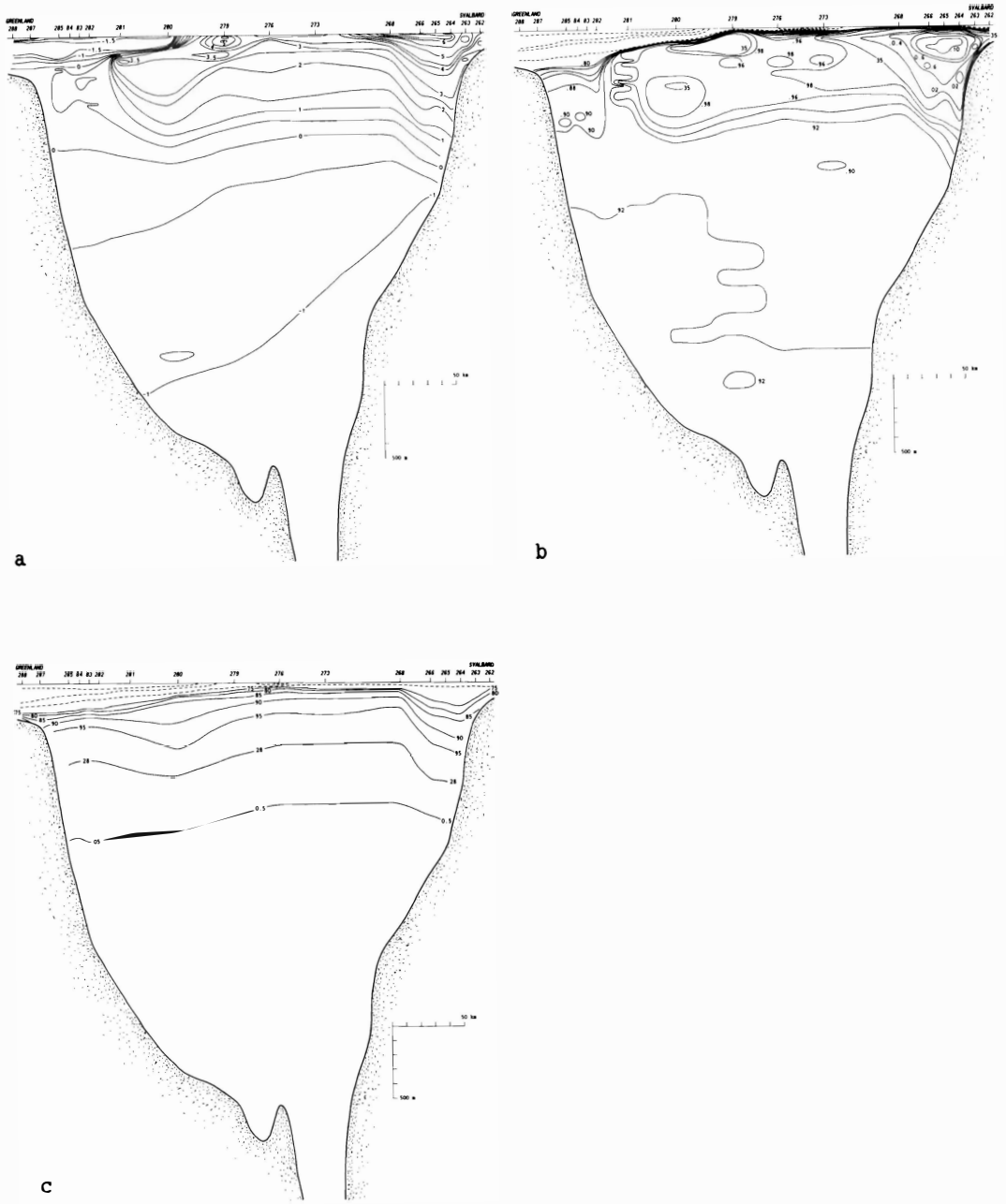

Fig. 5a–c. Sections of potential temperature, salinity and potential density: 'Lance' section.

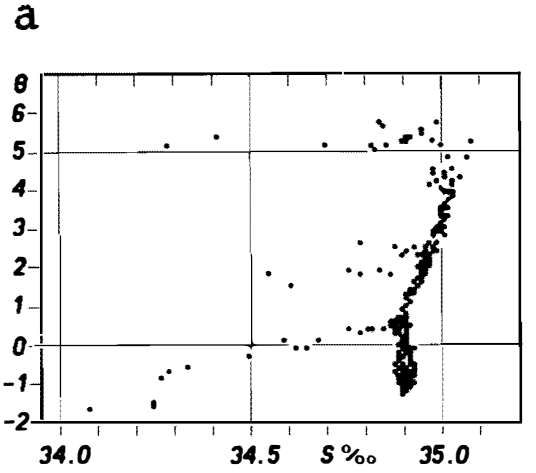

Fig. 6a. θ–S diagrams for the 'Ymer' section: All stations. Water masses I–VI indicated.

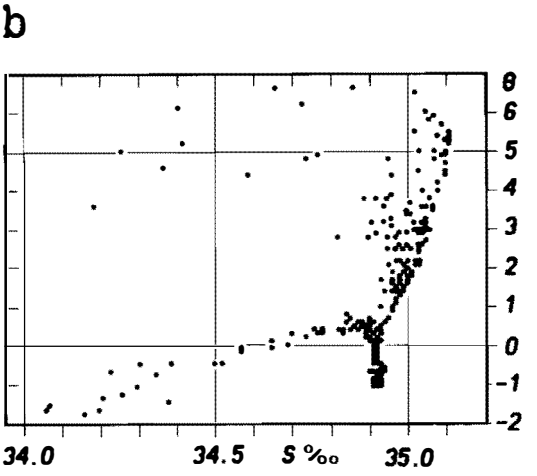

Fig. 6b. θ–S diagrams for the 'Lance' section: All stations. Water masses I–VI indicated.

VI, which in both sections are present everywhere except in the western part. There is a slight but significant cooling of these waters as we move towards the west. A probable explanation for this would be that we in the west observe AW, which is moving south after a short circulation in the northern part of the strait. The observed changes in the θ–S characteristics may result from mixing with the polar surface water above and perhaps also from direct cooling. Some changes may also be due to isopycnal mixing with water masses IV and IIa, and there are signs of interleaving in that density range in the central western part (Fig. 5a, b).

There are differences between the two years, the most significant being the warmer, saltier water found in the eastern part in 1983. This difference must result from interannual variations. The rather cold signature found for the water masses V and VI in the central eastern part in the 1983 section is, however, due to the presence of the Molloy Deep, which tends to diminish the vertical temperature and salinity gradients and display colder, fresher surface water and warmer, saltier deep water. The same feature was observed at a corresponding station over the Molloy Deep in 1980.

The water mass IV is observed over the entire cross section, and in the western part it constitutes a cold temperature maximum. The θ–S characteristics are very similar in this part in the two years, and the water mass found in this region probably indicates the return flow of AW, which has penetrated deep into the Polar Ocean and become modified by the thermodynamic processes active in the interior of the Polar Ocean. In the central and eastern part of the passage this interpretation of water mass IV becomes more doubtful. On the 1983 section it just represents a transition layer, while in 1980 it appears as a salinity minimum (Rudels & Andersson 1982). An extremum is by necessity an advective feature, and we need to locate a possible source for this minimum. In 1980 returning modified AW (class IV) could enter from the west into the central and eastern parts of the strait. Since a corresponding minimum is not found in the 1983 section, which has saltier class IV water in the central eastern areas, such events would be intermittent and probably triggered by some meteorological forcing.

Another, perhaps more likely explanation would be that this water mass is created to the

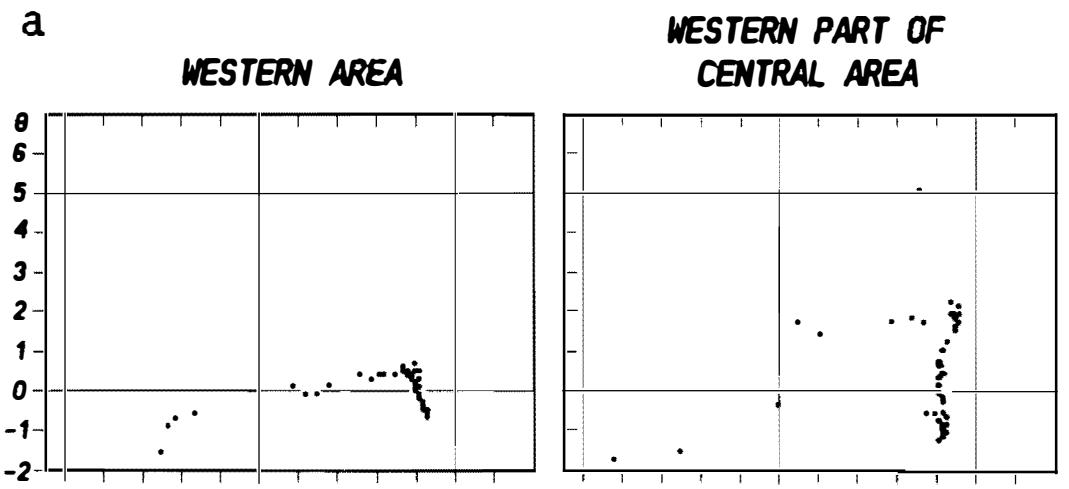

Fig. 7a. θ–S diagrams for the 'Ymer' section.

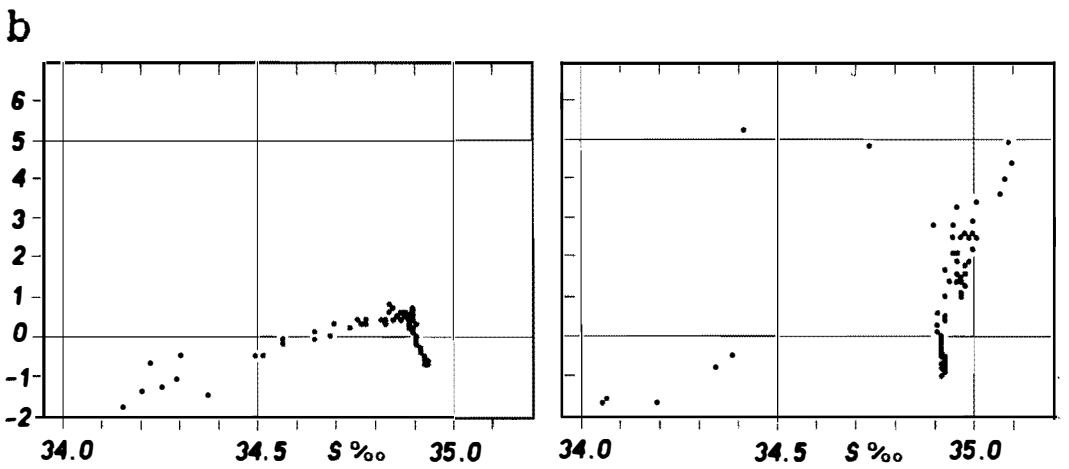

Fig. 7b. θ–S diagrams for the 'Lance' section.

a

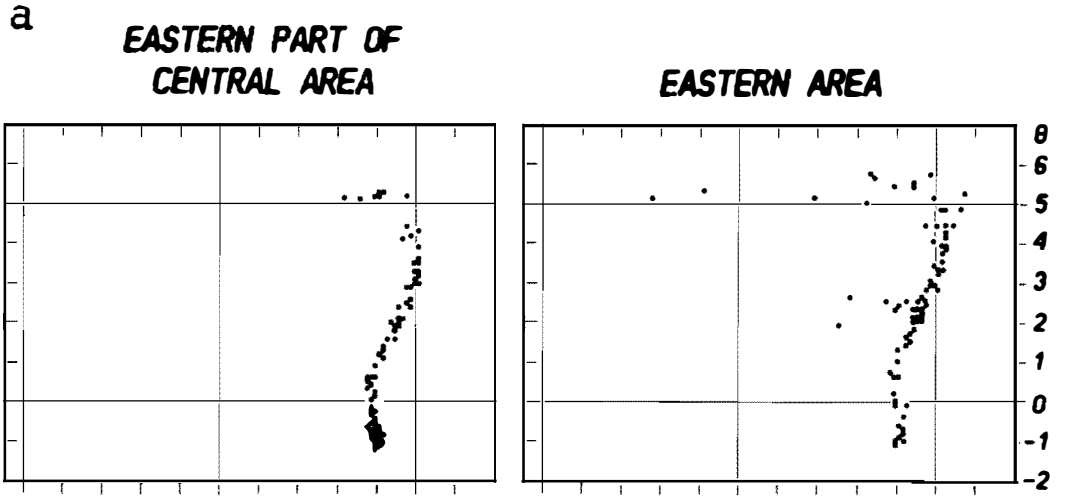
EASTERN PART OF CENTRAL AREA
EASTERN AREA
θ
6
5
4
3
2
1
0
-1
-2

b

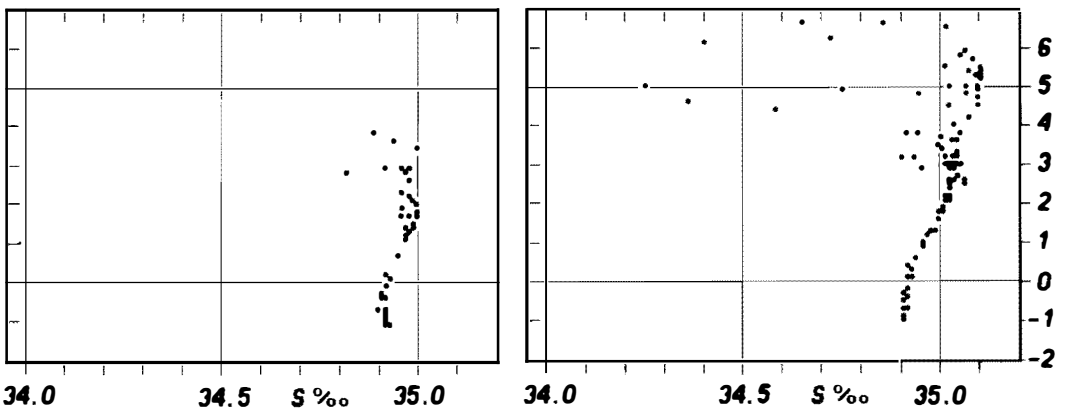
34.0
34.5
S ‰
35.0
34.0
34.5
S ‰
35.0
6
5
4
3
2
1
0
-1
-2

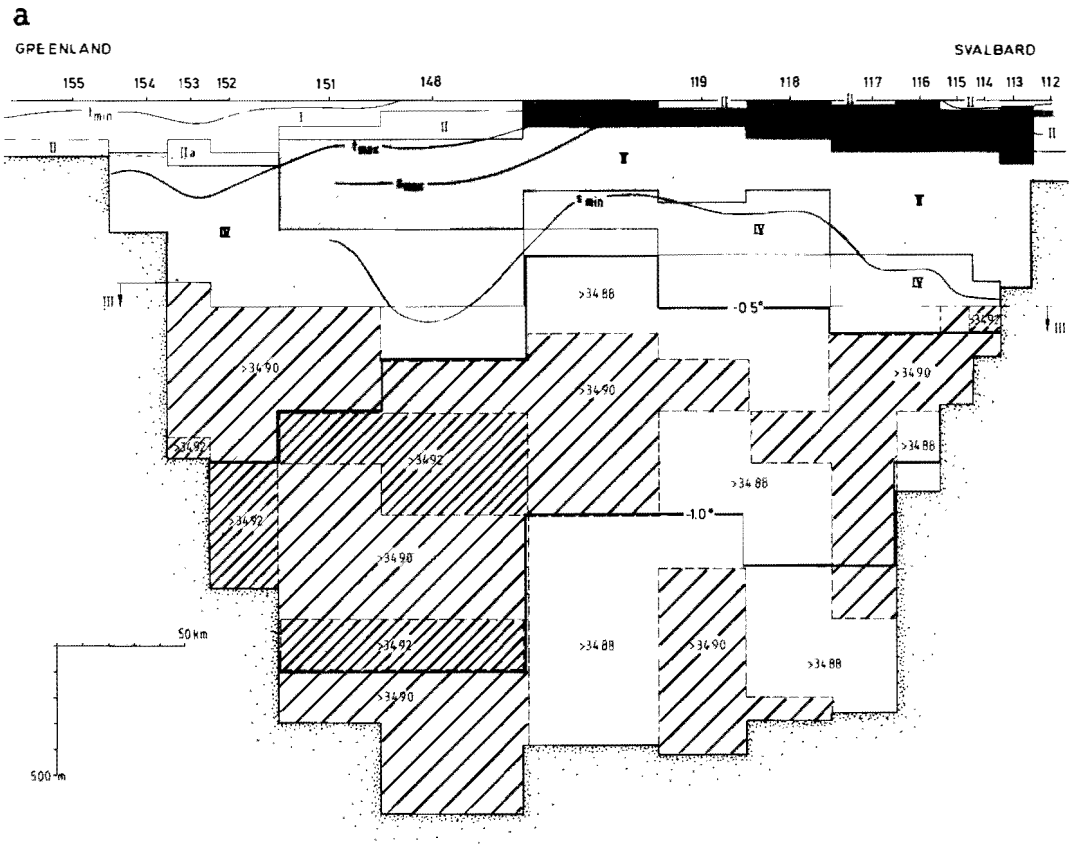

Fig. 8a. The distribution of water masses I–VI on the 'Ymer' section.

south, probably in the Greenland Sea, by cooling during the winter and then advected north into the Fram Strait. A colder $-0.5 < \theta < 0$ salinity minimum is observed in 1983, and the variation in temperature could be the result of different conditions prevailing in the Greenland Sea from year to year.

Water mass II and IIa includes warmer polar surface water and AW freshened by ice melt. On the eastern part of the section the Svalbard coastal water, which primarily derives from the Barents Sea and enters the Atlantic south of Sørkapp, shows up as class II water.

Finally water mass III represents all the deep and bottom waters. Here the partition is too coarse to distinguish between different contributions, and some elaboration is needed. The θ–S characteristics of the different deep waters (depth > 2000) have been compiled by Swift et al. (1983). They give GSDW: $-1.29 < \theta < -1.26$, $34.899 < S < 34.892$, NSDW: $-1.06 < \theta < -0.93$, $34.908 < S < 34.911$, and PODW: $-0.96 < \theta < -0.70$, $34.921 < S < 34.936$. The 'Ymer' and 'Lance' stations have slightly lower salinity (~ 0.004) in the

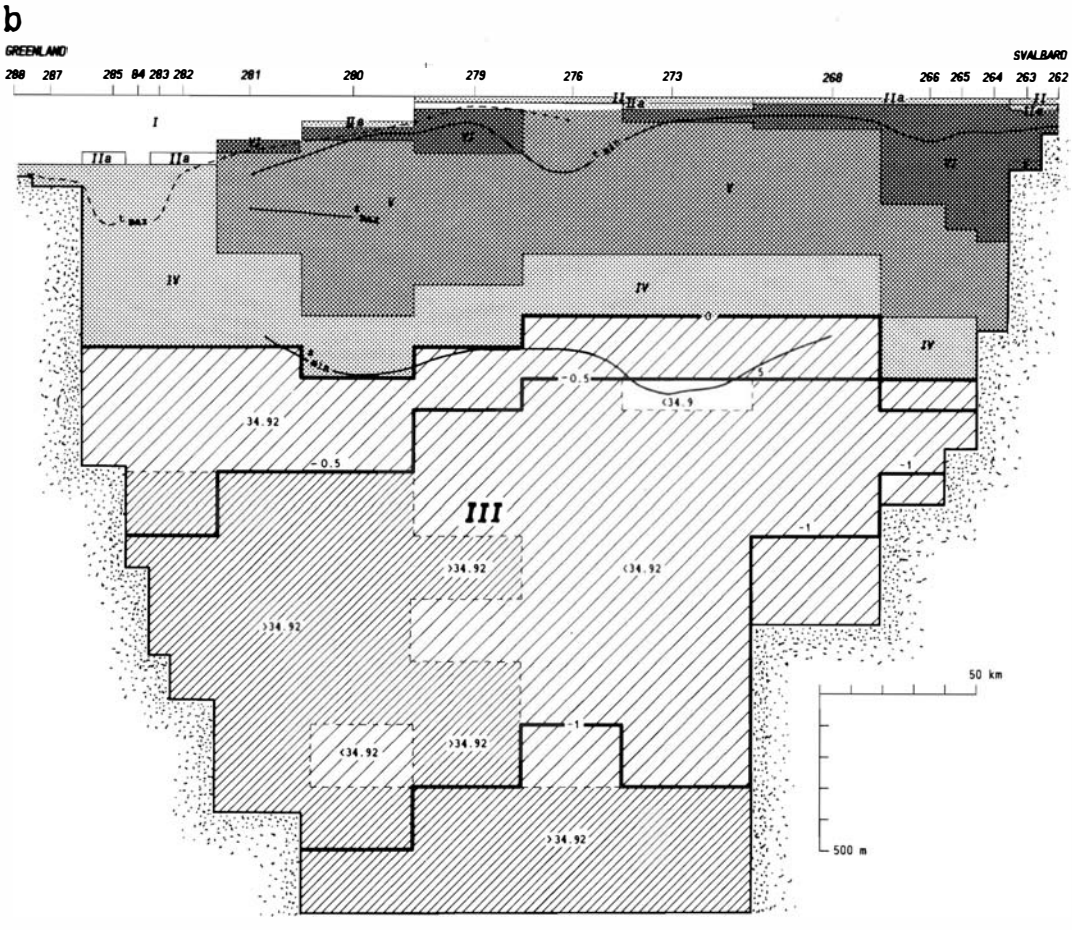

Fig. 8b. The distribution of water masses I–VI on the 'Lance' section.

NSDW, which is the only common water mass, and we consider such a departure acceptable for our present purpose.

The tendency is fairly clear. Colder, fresher deep water ought to have a southern origin, while warmer, saltier water masses should derive from the Polar Ocean. The transformation of the deep water masses is an intriguing question (Swift et al. 1983; Aagaard et al. 1985; Rudels 1986b), and here we just remark that the different θ–S signatures of GSDW and PODW are probably due to the different settings, where the cooling, ice formation, and brine rejection occur. In the Polar Ocean this happens over shallow areas with a thick warm Atlantic layer just off the shelf, while in the central Greenland Sea the depth is greater than 3000 m, and the Atlantic water is practically absent. The NSDW finally looks like a mixture between these two primary water masses (Aagaard et al. 1985; Rudels 1986b).

A look at the θ–S diagrams and at the sections reveals that most of the Polar ocean deep water is confined to the western part close to the Greenland continental slope, while in the

central and eastern parts GSDW and NSDW seem to dominate. Some reservations need to be made, especially for the western central part, where a direct mixing between PODW and GSDW may occur, and the ruggedness of the θ–S curves in the deeper layers indicates that this is the case (Rudels 1986b). The final mixing product will have the characteristics of NSDW.

We may also note that the water masses in the central and eastern parts of the cross section were warmer and more saline, especially close to the bottom, in 1983 compared to 1980. Whether these changes are normal interannual variations, or whether they are due to the more northerly position of the 'Lance' section, and the fact that we could not sample to the bottom in the central eastern part in 1983, cannot be decided with certainty. I favour the latter since there are signs of a rapid disappearance of the extreme GSDW characteristics towards the north (Rudels 1986b). Still, if the GSDW manages to cross the sill, it could, aided by the pressure effect on cold water, sink down towards the bottom of the Lena trough and there constitute a deep bottom layer.

Figs. 8a, b show the different water masses in the idealized cross sections and thus summarize the discussion given above. To display the gradients in the deep water mass (III) the isoterms –0.5, –1.0, and the isohalines 34.90, 34.92 have been drawn. The positions of extrema in temperature and salinity are also indicated.

We may note that the temperature and salinity maxima separate as we move towards the west. This is a feature which appears when an overlying cold low saline water mass mixes vertically with an underlying warm saline core, independent of the type of mixing. However, the separation is more pronounced with ordinary mechanical mixing than with dominantly double-diffusive mixing in the diffusive sense. It thus cannot be used as an indication of double-diffusive convection (Fig. 9). This is at odds with what is stated by Carmack & Aagaard (1973) in their work on the deep water formation in the Greenland Sea. However, the largest separation would occur if saltfinger convection into a lower less saline layer were present.

7.2. The baroclinic velocity field

We shall approximate the real bottom topography with a step profile, where the depth 'd_i' observed at station 'i' is taken to hold over the width 'b_i' of the station, which reaches halfway to the neighbouring stations 'i–1' and 'i + 1'. For the 1983 data the section has been terminated at 2600 m for the deepest stations, and no motion is assumed below this level in spite of the much greater depth of the Molloy Deep. Some horizontal interpolations have been made at the lower levels, where data were lacking (stn. 273, 276).

The water column at each station is partitioned into boxes of heights 'h_j'. The heights vary with depth but are equal at the same level for all stations (except for the box closest to the bottom). The chosen depth intervals and box heights are listed in Table 2.

The potential temperature θ_{ij} and salinity S_{ij} observed at midheight of box a_{ij} – with the area $a_{ij} = b_i \cdot h_j$ – are taken to hold for the entire box a_{ij}. The values θ_{ij}, S_{ij} were used in constructing the θ–S diagrams discussed above.

The baroclinic velocity field is first determined with respect to an arbitrary reference level. The dynamic heights are computed from the expression

$$D = \sum_{k=1}^{K} \frac{\varrho_{ok} - \varrho_k}{\varrho_{ok}\varrho_k} \Delta P_k$$

where ΔP_k is 2 db and $\frac{\rho_{ok} - \rho_k}{\rho_{ok}\,\rho_k}$ gives the average density anomaly for every two db interval.

When calculating the geostrophic velocities we obtain the velocity between two stations instead of at the station. However, we do not want to form average temperatures and

Fig. 9a. Changes in θ–S relation due to mechanical mixing.

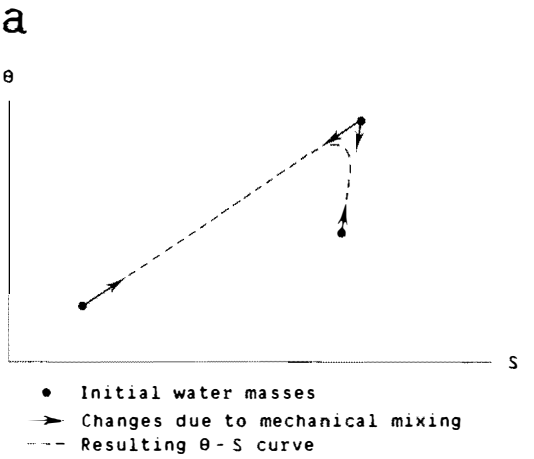

Fig. 9b. Changes in θ–S relation due to double diffusive convection: Diffusive interfaces and salt fingers.

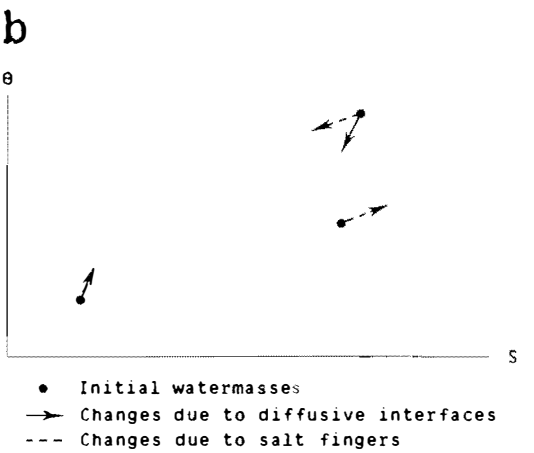

Fig. 9c. The resulting water column due to double diffusive convection.

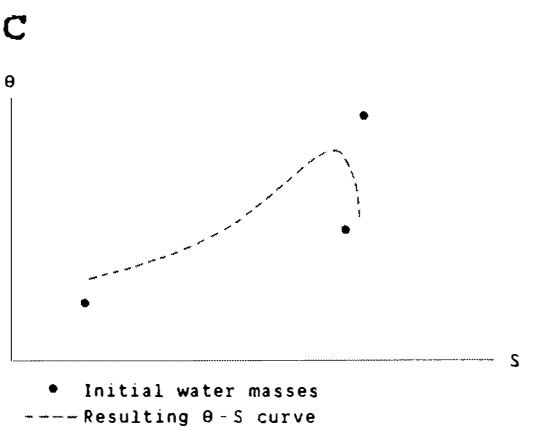

Table 2. Height of boxes a_{ij} on the two sections.

depth interval m	box height 'Ymer' m	box height 'Lance' m
0 < d < 100	20	20
100 < d < 500	50	40
500 < d < 100	100	100
1000 < d	200	200

salinities such as $^1/_2(\theta_{(i+1)j} + \theta_{ij})$ etc., but instead retain the observed values and the proposed partition of the sections into boxes a_{ij}. Our solution has been to introduce two velocities v'_{ij} in the right and v''_{ij} in the left part of the box a_{ij}. These velocities are then determined as usual from the differences in density anomaly between stations 'i–1' and 'i', and 'i' and 'i + 1' respectively.

Between stations of unequal depths an additional density anomaly Δ arises in the lower part of the deeper station. This anomaly is computed using the method of Jacobsen & Jensen (Fomin 1964). Because of the introduced step profile some modifications have been necessary. At the shallower stations, e.g. 'i', the additional density anomaly is zero at the bottom (level j), but at the deeper station 'i + 1' an additional anomaly

$$\Delta = 2^{-1}d(\alpha_{(i+1)j} - \alpha_{ij})$$

needs to be added to obtain the density anomaly at the bottom. α_{ij} denotes the specific volume at j, and d is the difference in depth between the two stations. Between the two bottom levels Δ is assumed to be a linear function of depth

$$\Delta(\zeta) = 2^{-1}\zeta(\alpha_{(i+1)j} - \alpha_{ij}) \quad 0 \leq \zeta < d$$

allowing for a linear shear in the deeper part (below level j) of station 'i + 1'. The profiles above this level are the same for the two stations except for their as yet unknown barotropic velocity components.

This correction, which arises because of the unequal depth of the stations, may be quite large and result in large errors in transports if the wrong reference level is chosen (see in particular stn. 117, Fig. 10a).

7.3. The barotropic velocity field and the variational approach

The velocity field in the Fram Strait is now determined up to an unknown barotropic part to be added to each station. These barotropic velocities are not arbitrary, but need to conform to constraints, which depend upon processes active in the Polar Ocean and in the Greenland and Norwegian Seas. The number of constraints that can be formed depends upon how well these processes are understood, and quite generally we may write

$$\int_A \varrho\delta_l(x,z)v(x,z)\,dx dz = C_l^0$$

$$l = 1, \ldots, L \qquad (1)$$

where A is the cross-section of the passage, v(x,z) is the total velocity, and C_l^* are the required constraints. $\delta_l(x,z)$ are dimension factors associated with the different constraints,

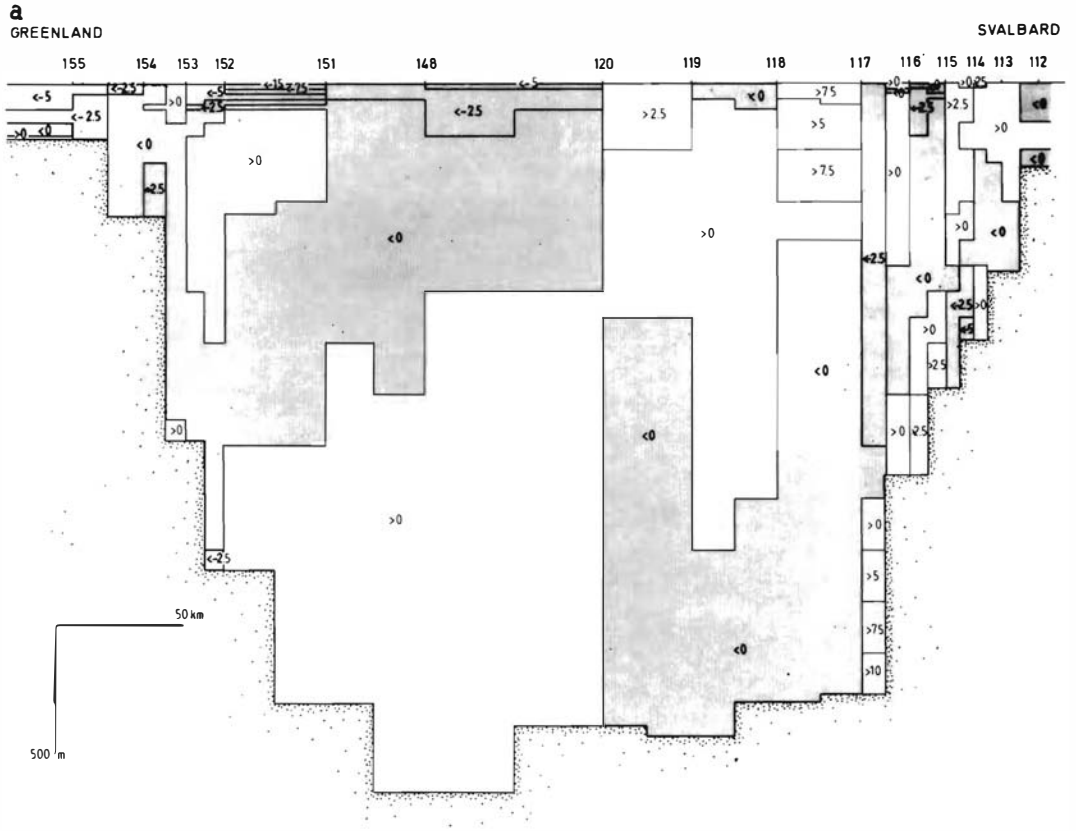

Fig. 10a. The velocity field in the Fram Strait: Mass and salt continuity required. 'Ymer' section. Positive flow towards the north. cm/s.

e.g. if C_l° represent the transport of salt through the Fram Strait, $\delta_l(x,z)$ would be the salinity on the cross section etc.

The velocity field consists of both the barotropic $v^b(x)$ and the baroclinic part $v^{bc}(x,z)$. We prefer to write the constraints as acting upon the unknown barotropic part. (1) then becomes

$$\int_A \varrho\delta_l(x,z)v^b(x)\,dxdz = C_l = C_l^0 - \int_A \varrho\delta_l(x,z)v^{bc}(x,z)\,dxdz$$

$$l = 1, \ldots, L \qquad (2)$$

and the contributions from the baroclinic field are thus included in the constraints.

In reality we are dealing with a discrete data set and the number (N) of undertermined barotropic velocities v^b depends on the number of stations. It will not require too many station pairs until the list of sensible constraints is exhausted, and the problem becomes underdetermined.

Some additional hypothesis is necessary, and we shall apply a 'principle of simplicity' as suggested by Claerbout (1976) and try to determine the least energetic flow through the

b

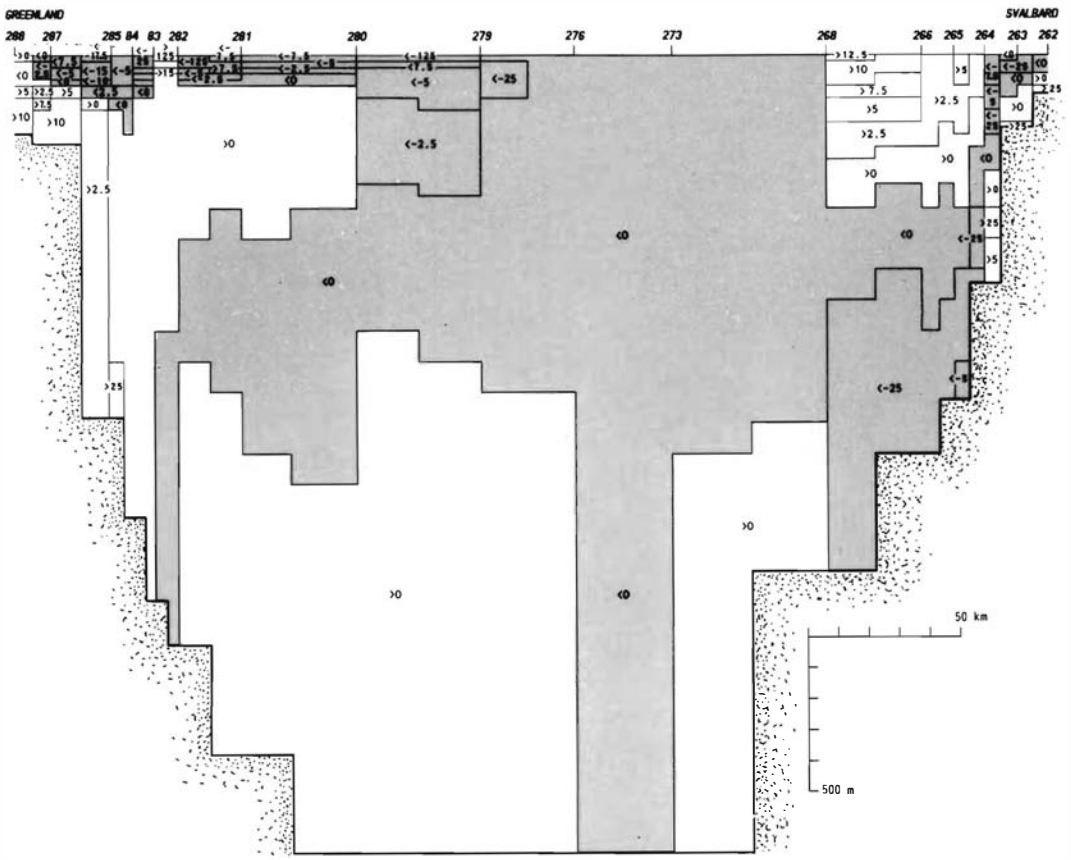

Fig. 10b. The velocity field in the Fram Strait: Mass and salt continuity required. 'Lance' section. Positive flow towards the north. cm/s.

Fram Strait capable of fulfilling the demanded constraints. Thus we shall minimize the integral

$$2^{-1} \int_A \varrho(v(x,z))^2 \, dx dz \tag{3}$$

which represents the total kinetic energy of the flow in the strait, subject to the constraints (2). We have chosen to minimize the kinetic energy associated with v(x,z) rather than the added barotropic kinetic energy

$$2^{-1} \int_A \varrho(v^b(x))^2 \, dx dz$$

since we then obtain a total velocity field, which is independent of the initial choice of reference level used to determine the baroclinic field. This is but one way to deal with the

uniqueness problem, and we refer to Fiadeiro & Veronis (1982), Wunsch (1978), Roemmich (1980) and Wunsch & Grant (1982) for thorough discussions of this problem and of the 'inverse' method in general.

To find the velocity field we shall pose a variational problem akin to that treated by Claerbout (1976, pp. 114–115) and those formulated by Stommel & Veronis (1981). Variation is performed on the barotropic velocity $v^b(x)$ in the intergral (3) subject to the constraints (2). Introducing the lagrangian multipliers λ_l we then have

$$\frac{\partial}{\partial v^b(x)}\left\{2^{-1}\int_A \varrho(v^b(x)+v^{bc}(x,z))^2\,dxdz+\sum_{l=1}^{L}\lambda_l\left(\int_A \varrho\delta_l(x,z)v^b(x)-C_l\right)\right\}=0 \tag{4}$$

By working with the kinetic energy, we automatically weigh the stations so that the cross areal dependence is removed. Changing to discrete notation equation (4) becomes

$$\frac{\partial}{\partial v_i^b}\left\{\sum_{i=1}^{N}\sum_{j=1}^{K(i)}2^{-1}\varrho a_{ij}(v_{ij}^{bc}+v_i^b)^2+\sum_{l=1}^{L}\lambda_l\left(\sum_{i=1}^{N}\sum_{j=1}^{K(i)}\varrho a_{ij}\delta_{ijl}v_i^b-C_l\right)\right\}=0$$

or

$$v_i^b\sum_{j=1}^{K(i)}\varrho a_{ij}+\sum_{j=1}^{K(i)}\varrho a_{ij}v_{ij}^{bc}+\sum_{l=1}^{L}\lambda_l\sum_{j=1}^{K(i)}\varrho a_{ij}\delta_{ijl}=0 \tag{5}$$

$i = 1, \ldots, N$

and the constraints are

$$\sum_{i=1}^{N}v_i^b\sum_{j=1}^{K(i)}\varrho a_{ij}\delta_{ijl}=C_l \tag{6}$$

where a_{ij} is the box area introduced above, and K(i) is the number of boxes at station i. Writing $a_i=\sum_{j=1}^{K(i)}\varrho a_{ij}$ and dividing all terms by a_i we obtain from (5)

$$v_i^b+a_i^{-1}\sum_{j=1}^{K(i)}\varrho a_{ij}v_{ij}^{bc}+\sum_{l=1}^{L}\lambda_l a_i^{-1}\sum_{j=1}^{K(i)}\varrho a_{ij}\delta_{ijl}=0$$

$i = 1, \ldots, N$ (7)

introducing the matrices

$$\mathbf{v}^b=\begin{bmatrix}\vdots\\ v_i^b\\ \vdots\end{bmatrix},\quad \mathbf{g}=\begin{bmatrix}\vdots\\ a_i^{-1}\sum_{j=1}^{K(i)}\varrho a_{ij}v_{ij}^{bc}\\ \vdots\end{bmatrix},\quad \mathbf{A}=\begin{bmatrix}\vdots\\ \cdots\sum_{j=1}^{K(i)}\varrho a_{ij}\delta_{ijl}\cdots\\ \vdots\end{bmatrix} \tag{8}$$

$$\mathbf{B}=\begin{bmatrix}\vdots\\ \cdots a_i^{-1}\sum_{j=1}^{K(i)}\varrho a_{ij}\delta_{ijl}\cdots\\ \vdots\end{bmatrix},\quad \mathbf{c}=\begin{bmatrix}\vdots\\ C_l\\ \vdots\end{bmatrix},\quad \Lambda=\begin{bmatrix}\vdots\\ \lambda_l\\ \vdots\end{bmatrix}$$

the equations can be written as

$$\mathbf{v}^b + \mathbf{g} + \mathbf{B}\Lambda = 0$$
$$\mathbf{A}^T\mathbf{v}^b = \mathbf{c} \qquad (9)$$

The lagrangian multipliers may be eliminated by inserting $\mathbf{v}^b$ into the second equation to obtain

$$-\mathbf{A}^T\mathbf{B}\Lambda - \mathbf{A}^T\mathbf{g} = \mathbf{c} \qquad (10)$$

which, when solved for the multipliers becomes

$$\Lambda = -(\mathbf{A}^T\mathbf{B})^{-1}\mathbf{c} - (\mathbf{A}^T\mathbf{B})^{-1}\mathbf{A}^T\mathbf{g} \qquad (11)$$

The barotropic velocities are then given by

$$\mathbf{v}^b = \mathbf{B}(\mathbf{A}^T\mathbf{B})^{-1}\mathbf{c} + \mathbf{B}(\mathbf{A}^T\mathbf{B})^{-1}\mathbf{A}^T\mathbf{g} - \mathbf{g} \qquad (12)$$

The resulting level of no motion is independent of the initial level used to compute the baroclinic field. The obtained *total* velocity field is unique, geostrophic, and fulfils the given constraints.

It is thus possible to eliminate some of the consequences arising from unfortunate initial choices. E.g. if a level of no motion was assumed incorrectly in the strong deep gradient on station 117 (Fig. 10a), a large barotropic correction would be needed to remove that error. If just the added barotropic kinetic energy were minimized, the system would try to keep the energy low by adding and substracting smaller velocities at the neighbouring stations. This is one reason why a choice of level of no motion in a velocity gradient will lead to small barotropic corrections when the inverse method is applied on the system and thus confirm the belief in a good initial guess. A guess which may well be mistaken.

Minimizing the total kinetic energy, however, has its own perils. If mixing between density surfaces is allowed, the system will generate solutions, which favour a vertical at the expense of a horizontal circulation. This is especially conspicuous when the baroclinic flow is strong enough to fulfil the constraints simply by adjusting the level of no motion and allow for bi-directional flow at each station. To be specific: If the circulation were horizontal with an inflow on one side and a corresponding outflow on the other side of the passage, and the flow contained a large baroclinic component, the solution with least total energy would be one of two superposed gyres, and such structures may thus be artifacts of the solution. If mass balance is required at different density intervals, these problems are eliminated.

These are but a few of the pitfalls and question marks which await us when we try to use the suggested minimizing approach, and the most difficult question may be to justify a search for a solution with minimum kinetic energy at all. Why should the velocity field be the weakest possible? We have no answer, but perhaps some excuses. Primarily: We are able to take advantage of a theory which has been developed and used since the time of Euler and Lagrange, and we do get an answer. Moreover, we also know that this answer is a lower bound. If the choices of constraints are sensible, the transports cannot be less than those we obtain.

7.4. Mass and salt balance in the Polar Ocean

The introduced constraints will be as general as possible to make them serve the dual purpose of 1) determining the transport through the Fram Strait and 2) giving information about the mixing processes in the interior of the Polar Ocean.

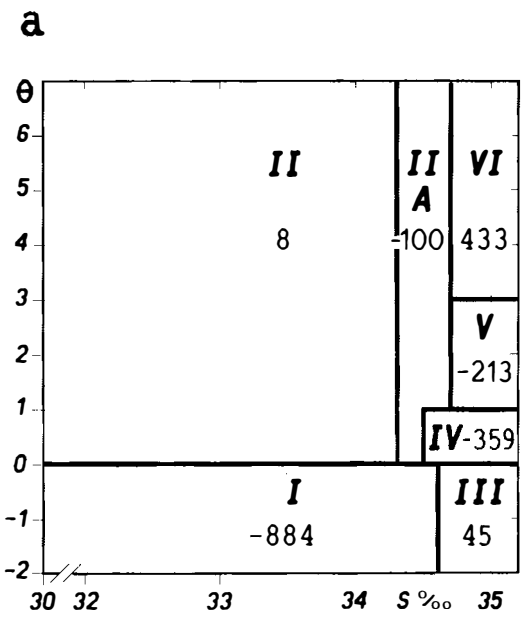

Fig. 11a. Transports of different water masses through the Fram Strait. 'Ymer' section. Mass and salt continuity required. Positive flow towards the north. 10^6 kg/s.

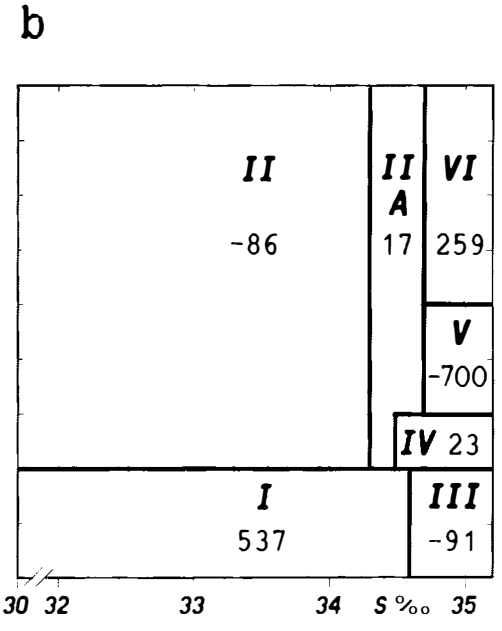

Fig. 11b. Transports of different water masses through the Fram Strait. 'Lance' section. Mass and salt continuity required. Positive flow towards the north. 10^6 kg/s.

Two obvious conditions which must hold are mass and salt balance. In the previous sections estimates have been obtained for the contributions from the other passages, and the flow through the Fram Strait must make up the difference. Heat balance could constitute another constraint, but for the Polar Ocean the oceanic heat flux is one important unknown which we hope to determine. The transformations of the water masses in the interior of the Polar Ocean also preclude any uncritical use of mass balance in distinct density intervals. We therefore choose initially to require only salt and mass balance for the entire Polar Ocean.

The constraints then take the form

$$\int_A \varrho v^b(x)\,dx dz = M_0 - \int_A \varrho v^{bc}(x,z)\,dx dz = M$$
$$\int_A \varrho S(x,z) v^b(x,z)\,dx dz = \phi_0 - \int_A \varrho S(x,z) v^{bc}(x,z)\,dx dz = \phi \qquad (13)$$

or in discrete notation

$$\sum_{i=1}^{N}\sum_{j=1}^{K(i)} \varrho a_{ij} v_i^b = M_0 - \sum_{i=1}^{N}\sum_{j=1}^{K(i)} \varrho a_{ij} v_{ij}^{bc} = M$$
$$\sum_{i=1}^{N}\sum_{j=1}^{K(i)} \varrho s_{ij} a_{ij} v_i^b = \phi_0 - \sum_{i=1}^{N}\sum_{j=1}^{K(i)} \varrho s_{ij} a_{ij} v_{ij}^{bc} = \phi \qquad (14)$$

introducing this into eq. (12) we then have

$$\mathbf{v}^b = \mathbf{B}(\mathbf{A}^T\mathbf{B})^{-1}\begin{bmatrix} M \\ \phi \end{bmatrix} + \mathbf{B}(\mathbf{A}^T\mathbf{B})^{-1}\mathbf{A}^T\mathbf{g} - \mathbf{g} \tag{15}$$

where

$$\mathbf{A} = \begin{bmatrix} \cdot & \cdot \\ \cdot & \cdot \\ \cdot & \cdot \\ a_i & s_i \\ \cdot & \cdot \\ \cdot & \cdot \\ \cdot & \cdot \end{bmatrix}, \quad \mathbf{B} = \begin{bmatrix} \cdot & \cdot \\ \cdot & \cdot \\ \cdot & \cdot \\ 1 & s_i a_i^{-1} \\ \cdot & \cdot \\ \cdot & \cdot \\ \cdot & \cdot \end{bmatrix} \tag{16}$$

and

$$a_i = \sum_{j=1}^{K(i)} \varrho a_{ij}, \quad s_i = \sum_{j=1}^{K(i)} \varrho s_{ij} a_{ij}$$

The barotropic velocities v_i^b may now be derived for the two sections and the estimated M_0, S_0 – the mass and salt transports through the other passages (Table 1).

The 1980 section includes a few stations on the Greenland shelf. These stations have been omitted, primarily to make the sections more compatible. There is, however, another reason. The few current measurements made on the shelf from the 'Ymer' (Rudels & Andersson 1982) indicated that the currents were dominated by tidal motions, and the ice and buoy drift through the Fram Strait also show a weak southward flow (Vinje 1983). If these shallow stations were included, the system might nevertheless export a large amount of the polar surface water over the shelf, since motions at these stations would add little to the total energy of the flow.

A run with the full 'Ymer' section departed not too conspicuously from what was found using stn. 112–155. A smaller outflow of Polar surface water was found, probably the result of lower salinities over the shelves. The flow of water mass IV over the Greenland slope was also reversed, which gave this solution somewhat smaller credibility than the one presented here (see disc. below).

The two velocity sections (Fig. 10) reflect the main current system. To the east the West Spitsbergen Current is present, but its structure is different in the two sections. In 1983 the core is rather compact and situated over the upper part of the slope to the east of the Molloy Deep. On the 'Ymer' section the current shows more structure and contains several cores, intertwined with return flows. To a large extent this may be due to the different topography of the two sections with the large protruding 1500 m deep plateau and the Molloy Deep present on the 'Lance' section. The westernmost core on the 1980 section may have been deflected towards the west and south already south of the latitude occupied by the 1983 section.

On the western side the velocity structures in the upper layers of the East Greenland Current are quite similar for the two years. The velocities and the eddy activities are, however, larger on the 'Lance' section. The strongest outflow is found over the deeper parts of the continental slope rather than close to the shelf break, consistent with what is observed from the ice and buoy drift in the Fram Strait (Vinje 1983; Vinje & Finnekåsa 1986).

At mid depths the velocity structures diverge. The unidirectional southward flow over the Molloy Deep and the continuous outflow layer found around 1000 m across the strait give the 'Lance' section a strange appearance. It should be kept in mind though that the velocities at stn. 119 in the 'Ymer' section are quite as small as those over the Molloy Deep in the 'Lance' section, and a weak barotropic velocity added to that station would result in a unidirectional flow from the surface to the bottom.

Beneath the upper 1000 m the sections are again similar with a northward flow in the west and a southward flow in the east. Close to and on the Svalbard slope a northward flow is found in both sections, albeit much stronger in the 'Ymer' section.

In 1980 almost the entire area over the Greenland slope constituted an outflow area, while in the 'Lance' section outflow was only found on a narrow strip. Both sections show the same eddy structure to the west at about 500 m, which is roughly in the area of the Atlantic return flow. The northward flow is much more prominent in 1983 and reaches the slope. The greatest differences between the two sections are accordingly found on the Greenland side.

Are the obtained flow fields realistic, or do they contain some systematic errors? Are the two different structures reasonable yearly variations, or is the solution for one or perhaps both of the sections unlikely? To form a better basis to judge these questions we shall compute and discuss the transports of different water masses through the strait.

Fig. 11 shows the transports of waters in the different θ–S intervals through the strait for the two sections. The most striking in these diagrams are the low values of the transports. Both the inflow of AW (V, VI) and the outflow of polar surface water (I) are well below what is commonly accepted. The largest transports of these water masses are found in the 'Ymer' section, while in the 'Lance' section we observe a strong outflow of water mass V, which, if correct, would indicate a large recirculation of warm AW in the northern vicinity of the Fram Strait.

Another difference is that there is no outflow in 1983 of the water masses IIa and IV, a θ–S range which we could expect to comprise the outflow of cold, modified AW from the Polar Ocean. The net circulation of the deeper water masses is in both instances close to zero.

However, these small figures may mask large transports in the different areas of the strait, and we shall look at how the transports are distributed over the cross section by making similar diagrams for the different parts of the strait. This is just a way to quantify and present information already present on the velocity section, which we believe is illuminating (Figs. 12a, b).

The transports of the warm water masses confirm the picture from the sections. The inflow of warm AW is concentrated to the eastern part in 1983, while in 1980 it was found in the eastern central area. The inflow is very low, and it is seen that most of it returns in both years only marginally cooled in the western central part. In 1983 this warm return flow is so strong that even an unrealistic total recirculation of the inflowing AW would not be enough to supply the computed outflow. In 1980 this outflow is weaker, and a net inflow to the Polar Ocean of $0.3 \cdot 10^9$ kg s^{-1} of warm AW seems to occur.

The water mass IV shows the largest variation between the two sections. Perhaps prematurely we expect this water mass to contain the outflow of modified AW, and on the 'Ymer' section a transport to the south is found in the western part. However, the 'Lance' section gives large northward flow in the same area.

The deep circulation is much stronger than the net flows suggest. Here too the transports found in 1980 conform better to what one would expect on the basis of the salinity distributions of the sections and in the Polar Ocean and in the Greenland/Norwegian Seas.

The discussion of the denser water masses can be further illuminated by forming the integrated transports for salinities > 34.7 for different temperature intervals as functions of salinity. The resulting curves for the entire sections as well as for the different parts of the sections are shown in Figs. 13, 14. The curves are terminated at the highest recorded salinity and then also indicate the salinity range of the transports in each temperature interval.

The warmer saltier characteristics of the water masses in 1983 are clearly revealed. Once

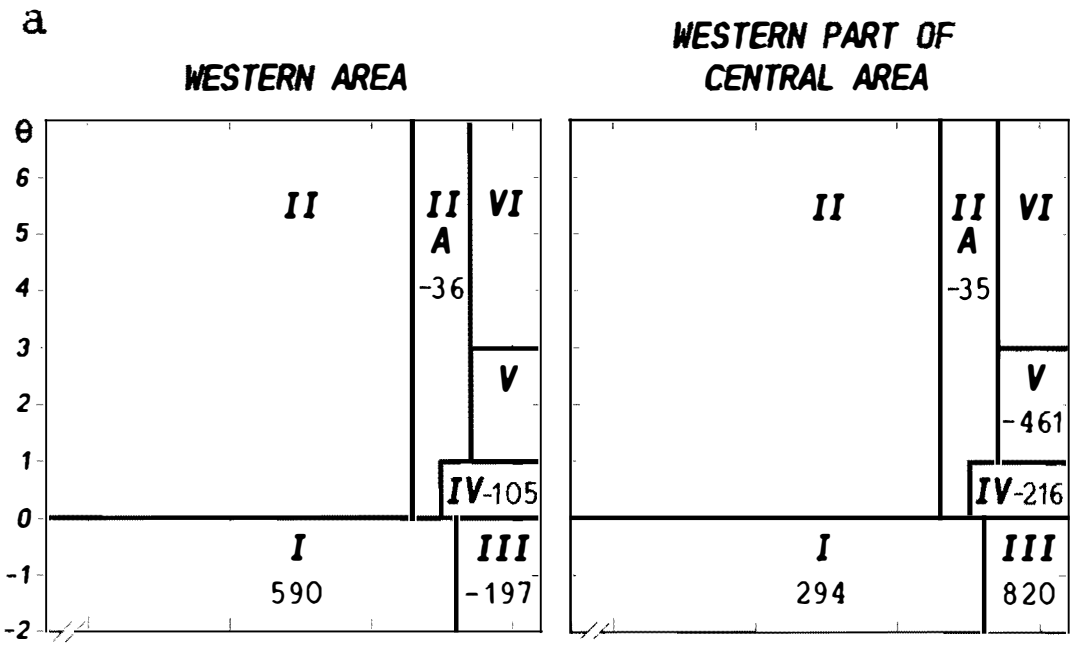

Fig. 12a. Transports of different water masses through parts of the cross section. 'Ymer' section. Mass and salt continuity required. Positive flow towards the north. 10^6 kg/s.

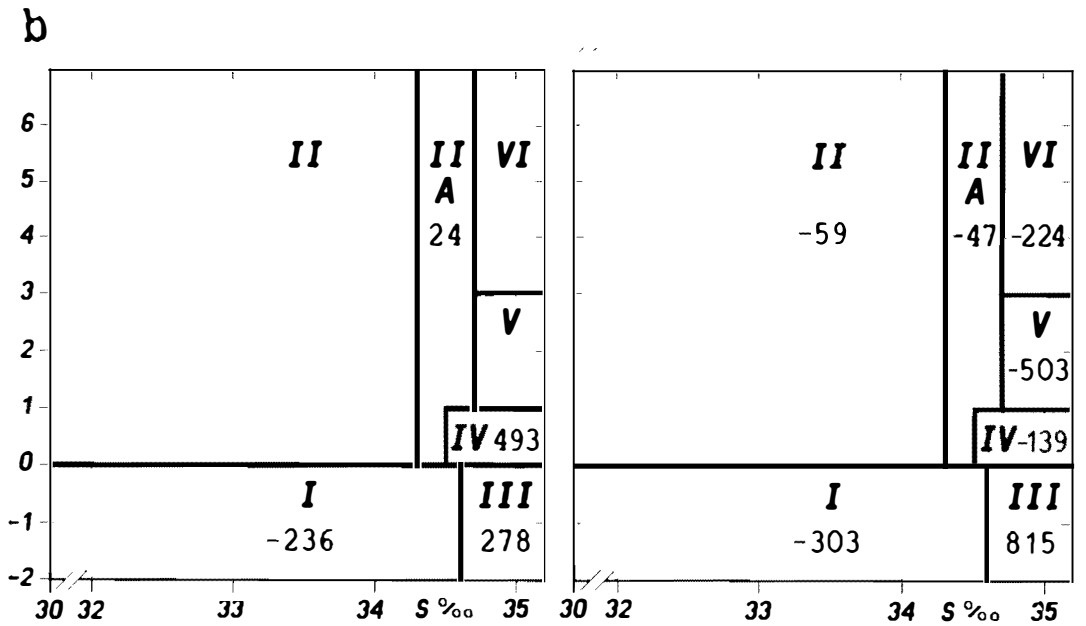

Fig. 12b. Transports of different water masses through parts of the cross section. 'Lance' section. Mass and salt continuity required. Positive flow towards the north. 10^6 kg/s.

a

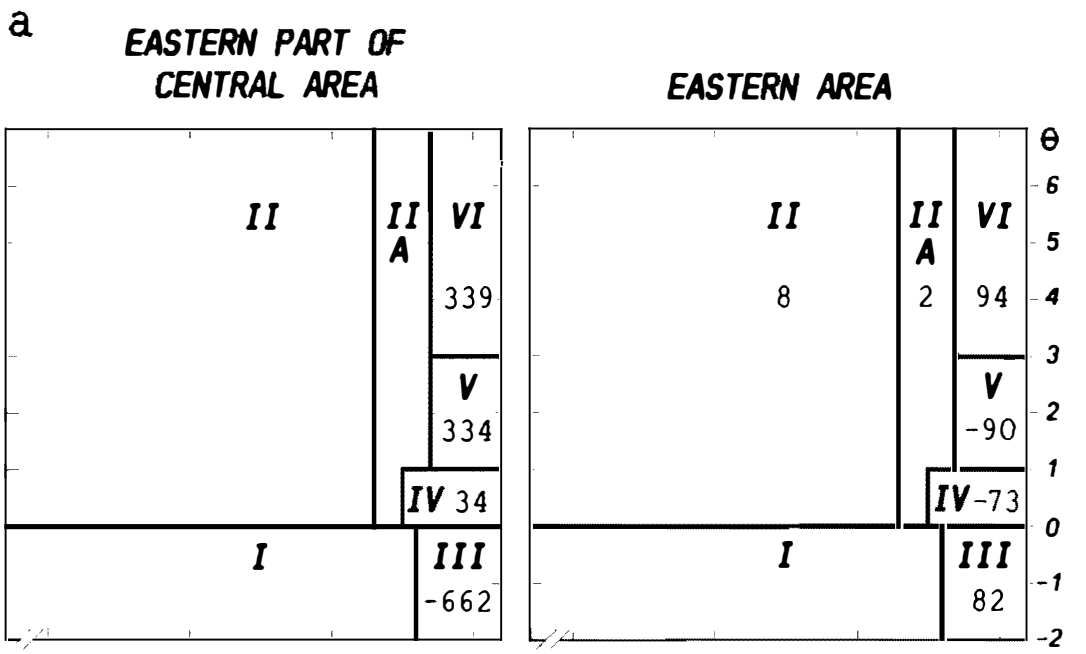
EASTERN PART OF CENTRAL AREA
EASTERN AREA
II
IIA
VI
339
V
334
IV 34
I
III
-662
II
8
IIA
2
VI
94
V
-90
IV -73
I
III
82
θ
6
5
4
3
2
1
0
-1
-2

b

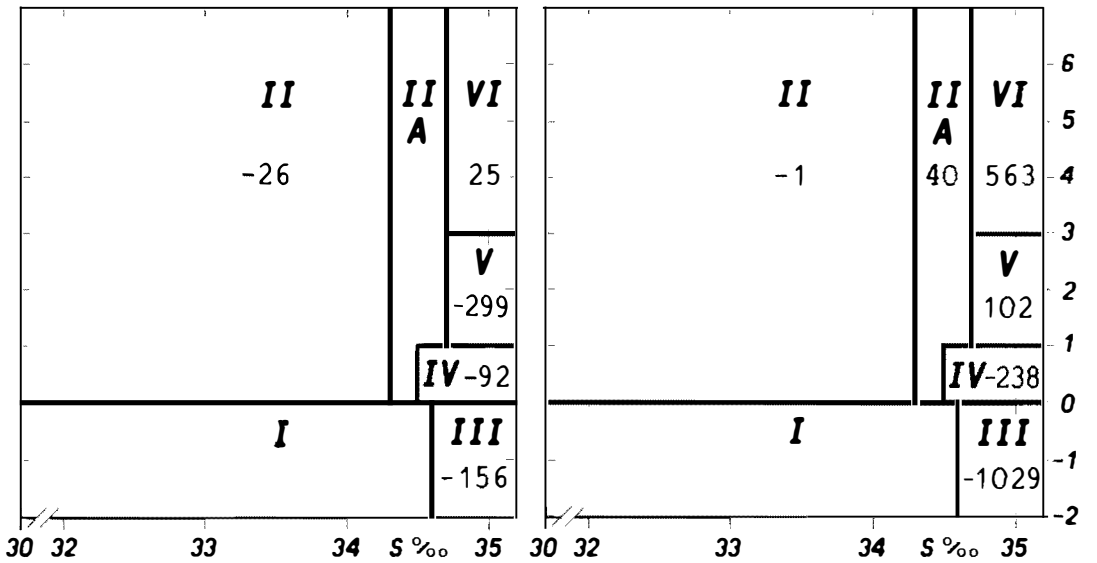
II
-26
IIA
VI
25
V
-299
IV -92
I
III
-156
II
-1
IIA
40
VI
563
V
102
IV -238
I
III
-1029
6
5
4
3
2
1
0
-1
-2
30 32 33 34 S ‰ 35
30 32 33 34 S ‰ 35

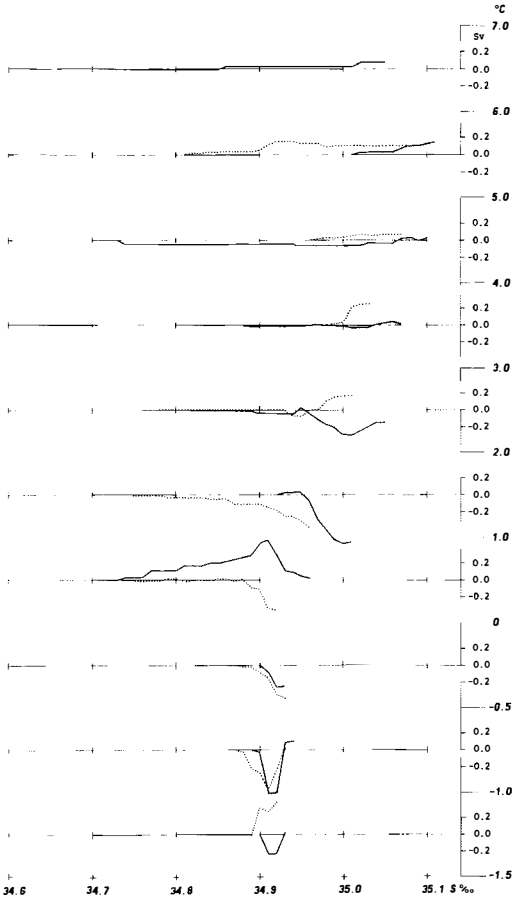

Fig. 13. Integrated transports through the entire cross section in different temperature intervals as functions of salinity, S > 34.7. Mass and salt continuity required. Positive flow towards the north. Dotted line: 'Ymer' section. Full line: 'Lance' section.

again we find the systematic trend of the inflow to occur at higher and the outflow at lower salinities; the only notable exceptions being the $0 < \theta < 1$ interval in 1983 and the cold, $\theta < -1$ water mass in 1980. The inflow in the coldest water mass is mainly that which takes place close to the Svalbard slope (stn. 117), and the inflow of water mass IV in 1983 is associated with the western area and appears to be questionable. While a saltier inflow and a fresher outflow are in accordance with the picture of the circulation in the upper layer, it is contrary to what should result from the salinity distributions in the deep waters of the Polar Ocean and the Greenland/Norwegian Seas.

In summary, the obtained solutions give transports that are small compared to other estimates (Table 5). The 'Ymer' section reveals a flow field, the structure of which is nearly compatible with what is known about the water mass properties of the surrounding sea. In 1983, however, a large part of the circulation is counter to these demands. Why is this so?

In the Polar Ocean two processes are active: The dilution of AW into Polar surface water, but also the formation of dense saline water, due to the brine rejection associated with freezing. This water enters the deeper layers and increases its salinity. The outflow through the Fram Strait is both fresher – in the upper layers – and saltier – in the deep and bottom layers – than the corresponding inflow.

When the least energetic flow is required, subject only to total mass and salt balance, a solution will be produced which has an inflow of AW, but also an inflow in the more saline part of the deep water mass, while the outflow is confined to the low saline parts of the cross section.

Since only barotropic velocities can be added to the given field, such a separation cannot be complete, but the solution will, as low salinity surface water is found above the more saline deep water to the west and saline Atlantic water above cold, fresh deep water to the east, create a vertical rather than a horizontal circulation. The solution tends towards a current field consisting of two superposed opposing gyres.

It is also clear that a large shear will enforce this feature, since the velocities in the upper layers will be played down by the requirement of the least energetic flow. The deeper water masses thus transport a larger part of the flow, leading to the paradox of a stronger baroclinic flow in the East Greenland Current resulting in a smaller southward transport of polar surface water. The weaker shears in the western part and perhaps also the strong deep inflow close to the Svalbard slope give the 'Ymer' section a more 'realistic' appearance than the 'Lance' section.

It is rather ironic that the strong shear, which occurs in the summer, acts to flaw the solution, while the smaller density differences present during the winter would give a total current field which better conforms to the known processes.

As things stand we would probably be better off if we had started arbitrarily with no velocity at the bottom and minimized the added barotropic field. However, we wish to retain the possibility of obtaining a unique solution not dependent on the initial choice of level of no motion, and we shall proceed using what is known or can be inferred about the deep water circulation.

7.5. Constraints on the deeper layers

What made us suspicious of the derived velocity fields was the transport of saline deep water into the Polar Ocean. The deep water in the Polar Ocean is more saline than in the Greenland/Norwegian Seas, and any realistic velocity distribution in the deeper layers should give a transport of saline water to the south.

This characteristic could be used to form additional constraints on the transports. It would require a knowledge of the inflow of deep water to the Polar Ocean and of the additional production which occurs in that ocean. In another paper (Rudels 1986b) I have tried to estimate these contributions from observed θ–S properties of the deep waters in the Greenland Sea, the Norwegian Sea, and the Polar Ocean. It was found that an inflow of $0.8 \cdot 10^9$ kg s^{-1} of NSDW with an average salinity of 34.905 and an outflow of PODW of $1.2 \cdot 10^9$ kg s^{-1} with the mean salinity 34.925 would be compatible with the observed changes. Below these deep exchanges will be introduced.*

We then form the additional constraints

$$\int_A \varrho v^b(x)\Gamma(S-S_0)\Gamma(T_0-T)\,dxdz = M_0^1 - \int_A \varrho v^{bc}(x,z)\Gamma(S-S_0)\Gamma(T_0-T)\,dxdz = M^1$$

$$\int_A \varrho v^b(x)S(x,z)\Gamma(S-S_0)\Gamma(T_0-T)\,dxdz = \phi_0^1 - \int_A \varrho v^{bc}(x,z)S(x,z)\Gamma(S-S_0)\Gamma(T_0-T)\,dxdz = \phi^1 \qquad (17)$$

with $\Gamma(S-S_0) = 1 \quad S>S_0 \quad S_0 = 34{,}8$

$\Gamma(S-S_0) = 0 \quad S<S_0$

and $\Gamma(T_0-T) = 1 \quad T_0>T \quad T_0 = 0\,^\circ\text{C}$

$\Gamma(T_0-T) = 0 \quad T_0<T$

* In a revison of the estimates (1986b) I have found the transports of NSDW and PODW to be 1.1 and $1.5 \cdot 10^9$ kg s^{-1} respectively. But these changes should not substantially affect the results obtained below.

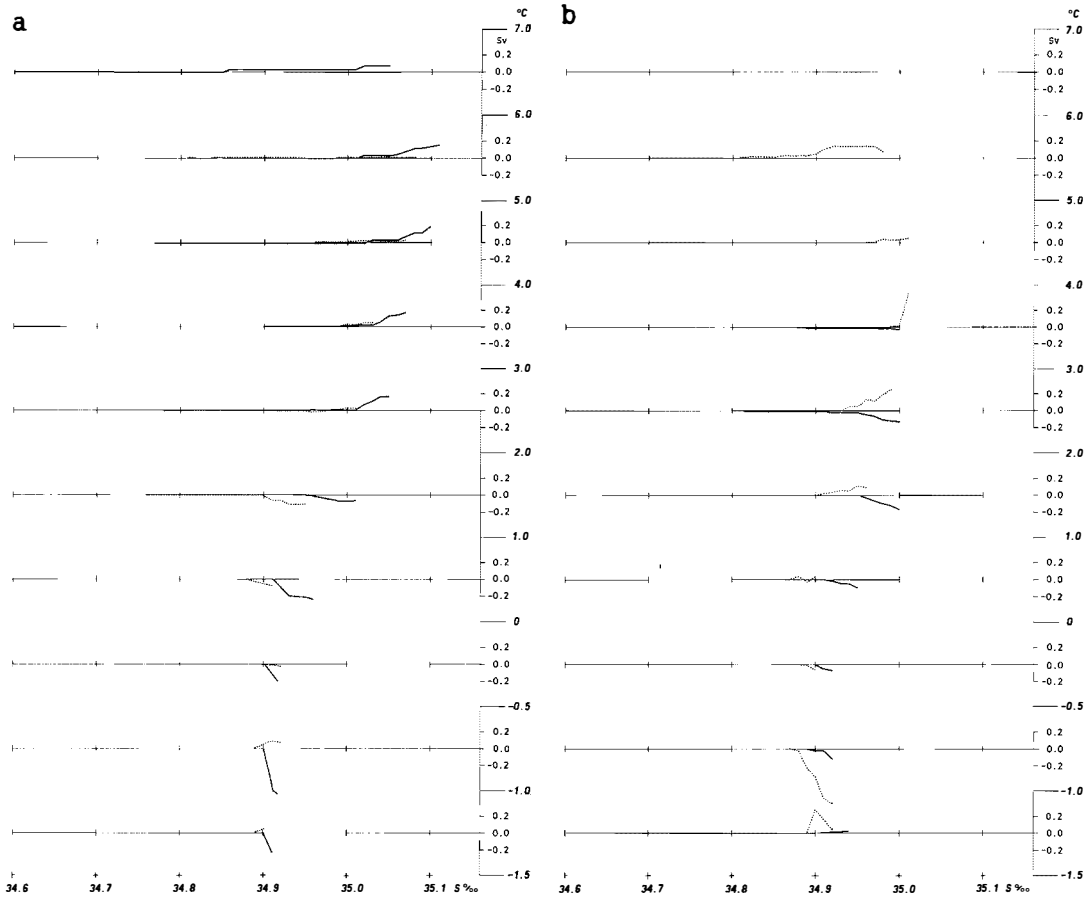

Fig. 14. Integrated transports through parts of the cross section in different temperature intervals as functions of salinity, S > 34.7. Mass and salt continuity required. Positive flow towards the north. Dotted line: 'Ymer' section. Full line: 'Lance' section. a) eastern part b) central eastern part c) central western part d) western part.

and where

$M_0' = -0.4 \cdot 10^9\,kg\,s^{-1}$ and

$_0' = (34.905 \cdot 0.8 - 34.925 \cdot 1.2) \cdot 10^6\,kg\,s^{-1}$

The main danger of introducing additional constraints is that the solution may be reduced to a mere tautological expression. However, by putting constraints on the deeper circulation, we are not seriously prescribing the oceanic heat transport, which occurs mainly in the upper layers, and we hope to obtain estimates of the transports of the upper water masses in the West Spitsbergen and in the East Greenland Currents as well as of the northward heatflux.

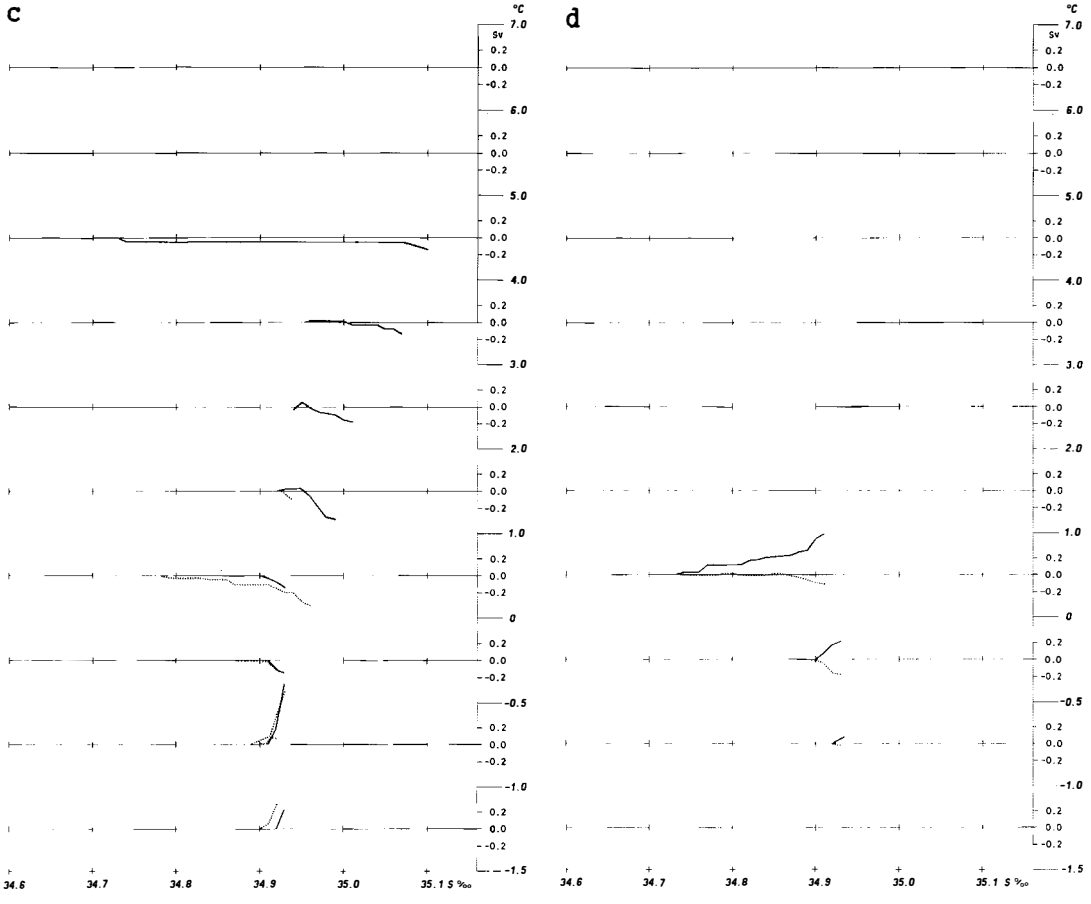

The equation for the barotropic velocities now becomes

$$\mathbf{v}^{\mathrm{b}} = \mathbf{B}(\mathbf{A}^{\mathrm{T}}\mathbf{B})^{-1}\begin{bmatrix} M \\ \phi \\ M^{1} \\ \phi^{1} \end{bmatrix} + \mathbf{B}(\mathbf{A}^{\mathrm{T}}\mathbf{B})^{-1}\mathbf{A}^{\mathrm{T}}\mathbf{g} - \mathbf{g} \tag{18}$$

where

$$\mathbf{A} = \begin{bmatrix} \vdots & \vdots & & \vdots & & \vdots \\ a_{\mathrm{i}} & s_{\mathrm{i}} & \sum_{j=1}^{K(i)} \varrho a_{\mathrm{ij}}\Gamma(S-S_0)\Gamma(T_0-T) & & \sum_{j=1}^{K(i)} \varrho a_{\mathrm{ij}}s_{\mathrm{ij}}\Gamma(S-S_0)\Gamma(T_0-T) & \\ \vdots & \vdots & & \vdots & & \vdots \end{bmatrix}$$

and (19)

$$\mathbf{B} = \begin{bmatrix} \vdots & \vdots & & \vdots & & \vdots \\ 1 & a_{\mathrm{i}}^{-1}s_{\mathrm{i}} & a_{\mathrm{i}}^{-1}\sum_{j=1}^{K(i)} \varrho a_{\mathrm{ij}}\Gamma(S-S_0)\Gamma(T_0-T) & & a_{\mathrm{i}}^{-1}\sum_{j=1}^{K(i)} \varrho a_{\mathrm{ij}}s_{\mathrm{ij}}\Gamma(S-S_0)\Gamma(T_0-T) & \\ \vdots & \vdots & & \vdots & & \vdots \end{bmatrix}$$

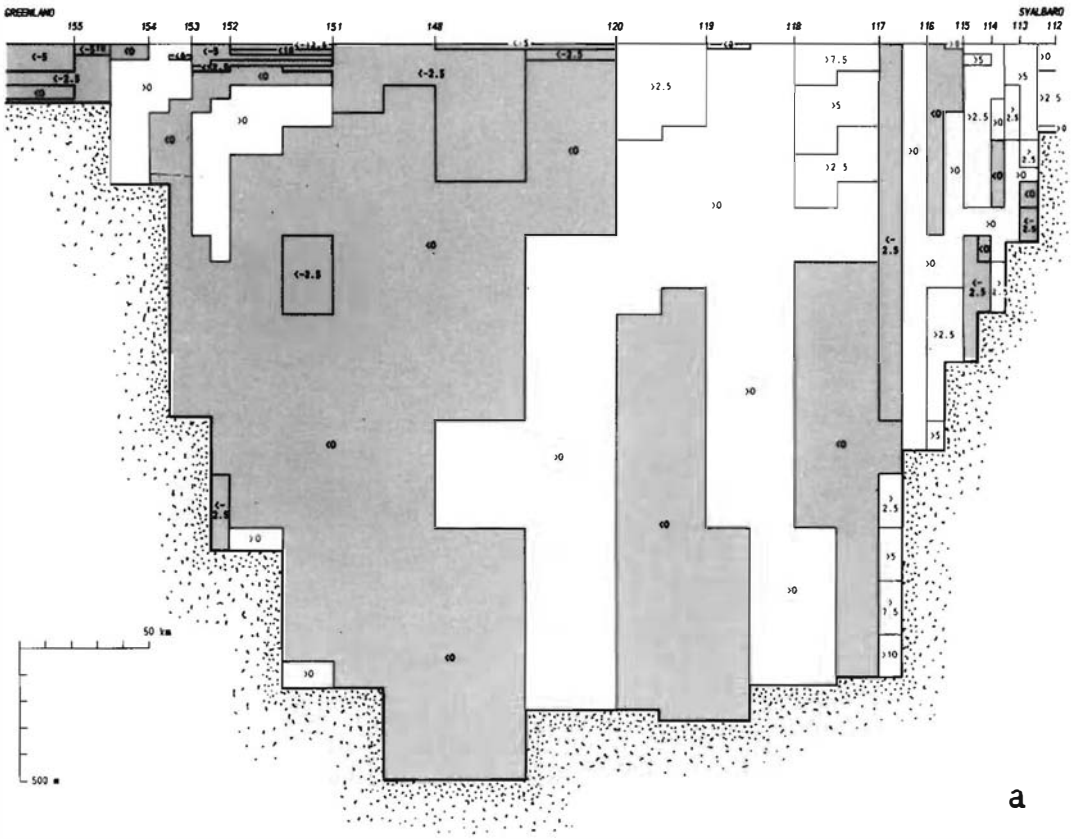

Fig. 15. The velocity field in the Fram Strait constraints on lower layer in addition to mass and salt continuity. Positive flow towards the north. cm/s.
a) 'Ymer' section.
b) 'Lance' section.

The resulting velocity fields are shown in Fig. 15.

The characteristic double gyre structure of the flow field, which was found earlier, has now largely disappeared, and the velocity field is more neatly divided into a predominantly northward flow on the eastern and a southward flow on the western side. But this picture is far from exhaustive, and in several instances motions against these main directions occur. In the deeper part of the basin there is a deep outflow situated close to the Molloy Deep, and further to the west a northward moving core is found. Over the continental slopes the flow direction is alternating between south and north, and the motions are suggestive of topographically trapped waves and eddies.

The structure of the flow fields in the two sections is quite similar, and the principal differences are again found over the Greenland shelf and the upper part of the slope. In both sections there are two northward moving cores, one attached to the continental slope and the other further to the east associated with the Atlantic water. The eastern core is more prominent in the 1980 section, where the northward flow close to the slope is weak. The opposite hold for the 1983 section. The northward flow to the west is here quite strong and completely dominates the motions over the upper part of the slope. Such a strong inflow in this area is contrary to what is expected, and again we shall examine if such a flow is consistent with the known water mass distributions.

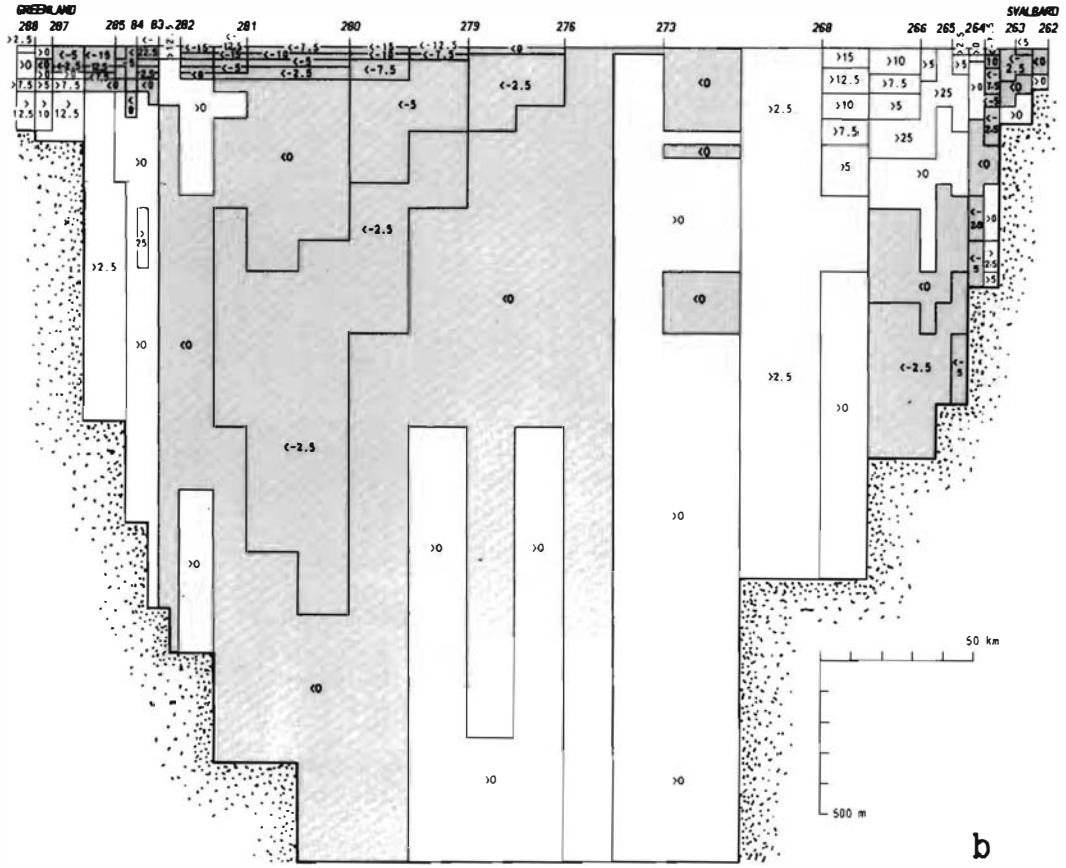

Forming the integrated transports as functions of salinity in different temperature intervals, we notice that the distribution of the transports in the colder water masses ($\theta < 0$) has changed due to the added constraints. The inflows now occur at lower and the outflows at higher salinities in the entire deep water mass (Fig. 16), and, as before, the outflows are found to be warmer than the inflows. This is in accordance with the required increase in salinity, and it implies an increase in temperature of the lower layers in the interior of the Polar Ocean, which is observed.

In the warmer water masses the differences between the two sections persist. In the $0 < \theta < 1$ interval the 1983 section indicates an inflow, while an outflow is found in 1980, and the transport functions formed for different parts of the sections (Fig. 17) show that the circulation of this water mass is different for the two sections, cyclonic in 1980 and anticyclonic in 1983.

Except for the interval $0 < \theta < 1$ in 1983 the outflow of water masses with temperature above 0 occurs in both sections consistently at lower salinities than the inflow, and the net transports change from an outflow in the lower temperature range towards an inflow as the temperature increases. This is in accordance with a freshening and cooling of the AW before it returns towards the south.

The transports in the different parts of the strait indicate that a cyclonic gyre dominates the motion over the entire passage, from surface to bottom, as is also seen from the velocity sections.

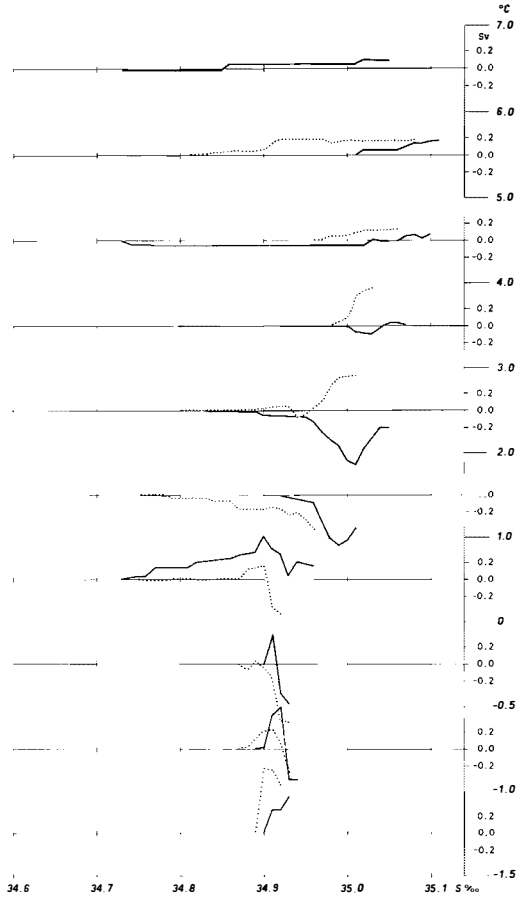

Fig. 16. Integrated transports through the entire cross section in different temperature intervals as functions of salinity, S > 34.7. Mass and salt continuity required and constraints on the deeper layers applied. Positive flow towards the north. Dotted line: 'Ymer' section. Full line: 'Lance' section.

The results obtained with the deep water constraints conform better with our prejudices about the flow field, but the discrepancy between the sections, which is especially evident by the different circulations found for water mass IV – the returning modified Atlantic water, is quite critical. It is also clear that not enough warm Atlantic water is transported into the Polar Ocean to sustain the strong southward flow found in the 1983 section for the interval $1 < \theta < 4$.

In summary, the impression remains that the 'Ymer' section presents a possible and may be even a probable picture of the current field and the transports, while the same approach applied to the 'Lance' section gives unrealistic results. However, we cannot discard a solution simply because we do not like what we get. Is there any objective reason for obtaining a better result in 1980 than in 1983?

The constraints which have been used are based upon what is believed to be average conditions holding for the Polar Ocean. The sections, however, are instantaneous pictures taken during the summer, when a substantial part of the ice cover has melted and a low saline surface layer is present. The baroclinic field is strengthened, but the additional freshwater has not been considered in the constraints. A strong baroclinic flow in the East Greenland Current may then exhaust the freshwater supply. This cannot happen, and the solution shifts the outflow to the more saline stations in the central western area. If the

baroclinic flow is sufficiently strong, it requires a compensating moderately saline return flow which must occur over the Greenland slope. The water mass IV, which we have reason to believe is AW leaving the basin, is thus forced by the solution to move north in the 1983 section because of the strong shears which are present in that year.

Since the condition pertaining for most of the year is one with smaller density differences we might expect the weak shears on the 1980 section to conform better with the annual average and give the result closest to the mean flow field and transports. However, it might still be quite different from the average conditions, and we shall not know for certain until sections taken in other seasons of the year are available. However, some conclusion of how the solution might be distorted with respect to reality may be drawn.

Because more freshwater is present in the water column than is accounted for by the constraints, the return flow will be located more towards the centre of the strait. The recirculation of warm AW in the passage will then be overemphasized at the expense of the AW which penetrates into the interior of the Polar Ocean north of Svalbard. If and in what way it will affect the northward flow in the West Spitsbergen Current is less clear, and we shall leave the speculations at this point.

Finally we should be aware that the strong eddy activity and short term variations of the current field will change the density structure in the sections on time scales comparable to the cruises and thus contaminate the solutions. The only way to eliminate these effects is to work with a yearly averaged representative density field. Such a field is, however, not available at present. We summarize the flows of different water masses in the same manner as in section 7.4 (see Figs. 18, 19) and then proceed to discuss the obtained transports and compare the results with other estimates.

8. The transports through the Fram Strait

To simplify the comparison of our estimates with other works the eastern and central eastern parts have been combined to comprise the West Spitsbergen Current, while the central western and western areas are taken to represent the East Greenland Current. The results for the different years and cases are shown in Table 3. In the West Spitsbergen Current just two water masses are distinguished: The Atlantic water (water masses II, IV, V and VI) and the deep water (III). The upper layers in the East Greenland Current are subdivided into polar surface water (I), Atlantic water (V, VI and the IIa water found on the western central area), and modified Atlantic water (IV and the IIa water observed in the western part).

The transport of Atlantic water obtained in the West Spitsbergen Current, when only mass and salt balance are required, is conspicuously small, and in 1983 there is even a southward flow of Atlantic water. The direction of the deep water circulation is contrary to what is intuitively felt to be true and also against the existing salinity distributions in the surrounding seas (sect. 7). The export of polar surface water in the East Greenland Current in the two sections is small but plausible, and the combined outflow of Atlantic and modified Atlantic water looks reasonable too.

When constraints are applied to the deep circulation a different picture emerges. The discrepancies between the two years have been dealt with at length above. It is interesting that the total transports in the upper layers of both the West Spitsbergen Current and the East Greenland Current only differ with less than 25% in spite of the different structures of the flows. As expected, the deep circulation is almost identical for the two years. The in- and outflows are somewhat higher than prescribed, a price necessary to pay for obtaining balance. The higher values may represent a real recirculation of deep water in the strait.

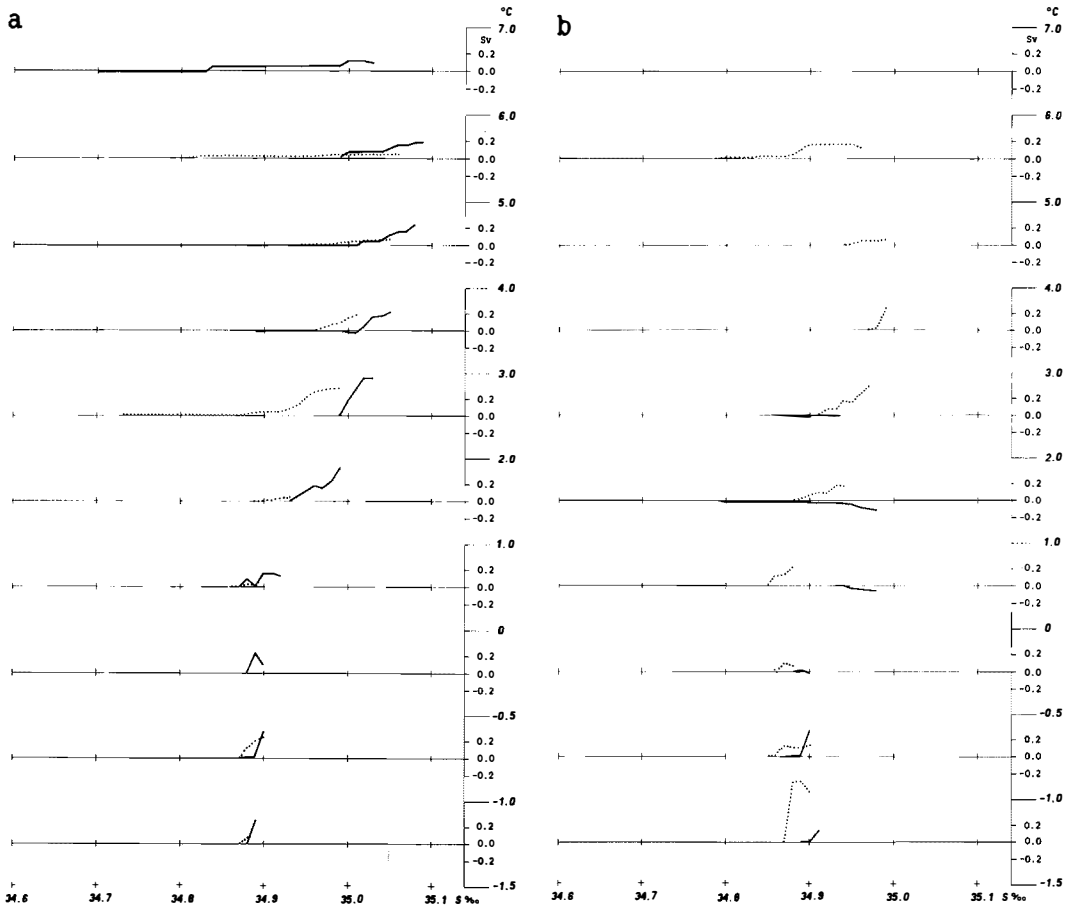

Fig. 17. Integrated transports through parts of the cross section in different temperature intervals as functions of salinity, S > 34.7. Mass and salt continuity required and constraints on the deeper layers applied. Positive flow towards the north.
Dotted line: 'Ymer' section. Full line: 'Lance' section. a) eastern part b) central eastern part c) central western part d) western part.

In the following we shall confine our discussion to the 'Ymer' section with the deep water constraints applied, which we consider by reasons given in the preceding section to be the one most representative of the prevailing situation.

The northward flow of AW in the West Spitsbergen Current is $1.9 \cdot 10^9$ kg s^{-1}. Half of this water mass recirculates in the strait or in its immediate northern vicinity and returns as warm AW in the EGC. The other half enters the Polar Ocean either directly north of Svalbard or north of the Yermak Plateau (Perkin & Lewis 1984). Part of this Atlantic water, together with the inflow over the Barents Sea, the Bering Strait inflow and the freshwater input, form the polar surface layer.

The heat loss experienced by the Atlantic layer could to a large extent be the result of cold, intruding dense plumes rather than mechanical mixing with overlying waters. The conserved or slightly increased density of the Atlantic water as it moves around the basin

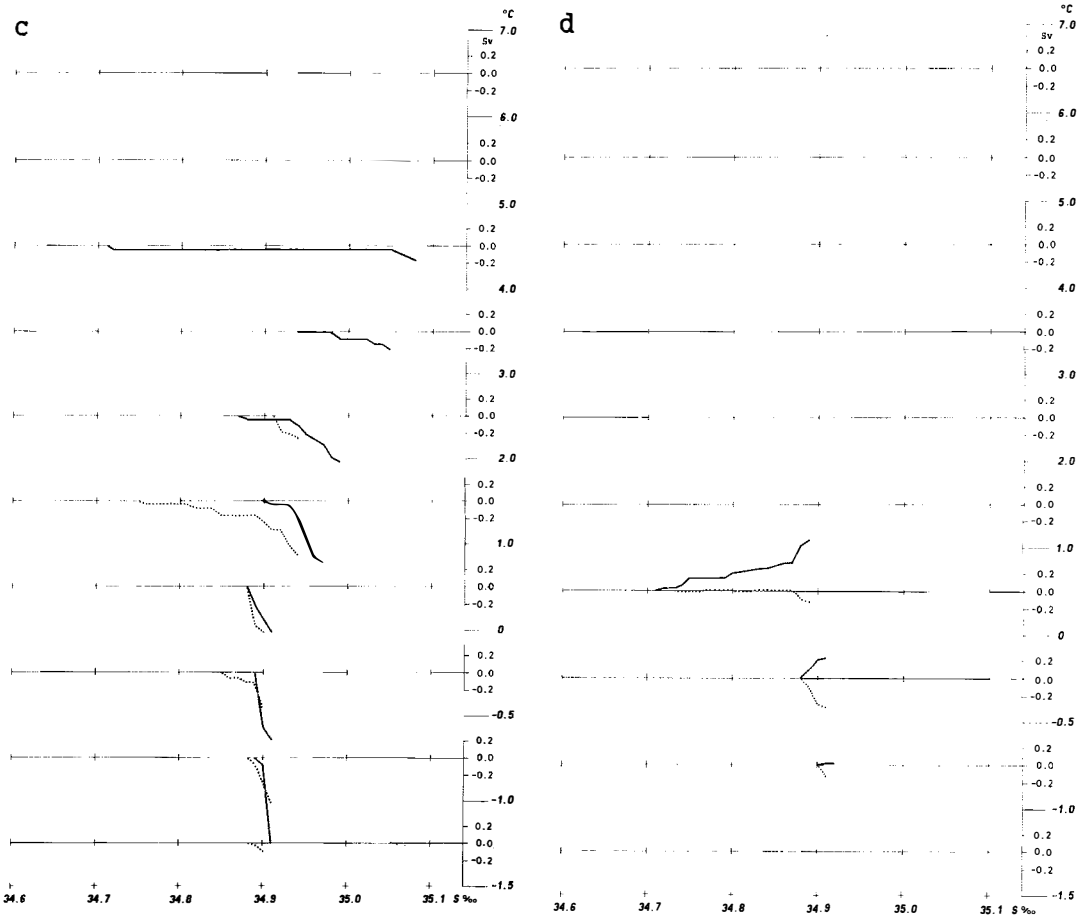

(SCOR-WG 58 1979) appears to confirm this. The increase in density might be due to double-diffusive processes, in this case diffusive interfaces. The outflow in the East Greenland Current consists of slightly less than $1 \cdot 10^9$ kg s^{-1} of PSW and $0.7 \cdot 10^9$ kg s^{-1} of modified Atlantic water. The recirculation of Atlantic water in the strait is thus comparably strong and comprises more than 1/3 of the flow in the upper layers of the East Greenland Current. Due primarily to this large recirculation of AW in the strait, the obtained oceanic heat transport is quite small, and the ice export carries a significant part of the oceanic heat flux (Table 4).

Some other efforts to establish mass and heat balances for the Polar Ocean are shown in Table 5. There is no point in discussing these estimates in detail as good reviews are found in Aagaard & Greisman (1975) and SCOR-WG 58 (1979). Quite generally, by comparison our results look small, but plausible. Two studies, though, warrant a closer

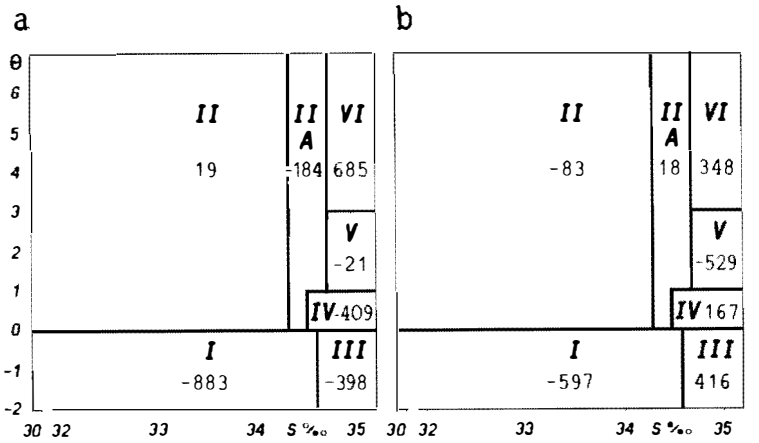

Fig. 18. Transports of different water masses through the Fram Strait. Mass and salt continuity required and constraints on the lower layers applied. Positive flow towards the north. a) 'Ymer' section. b) 'Lance' section. kg/s.

look, since they have a particular bearing on our work: 1) The paper by Östlund & Hut (1984), where freshwater balances obtained from isotope studies are used to establish the outflow in the upper layers. 2) The transport computations for the West Spitsbergen Current by Hanzlick (1983) based upon direct current measurements.

The isotope work by Östlund & Hut is very elegant. Their estimate of the total outflow through both the Fram Strait and the Arctic Archipelago and the combined inflow from the Atlantic and through the Bering Strait are within the range of most estimates and perhaps 30% higher than ours.

However, the most important discrepancy is the much larger ice export, which results from these computations. This is accompanied by a larger freshwater content in the water column due to a higher river run off and/or a larger inflow through the Bering Strait. If these values of the available freshwater are correct it would affect our transport estimates in the Fram Strait. The East Greenland Current would become stronger, and the transports would be shifted towards the low saline stations further to the west, perhaps also giving the 1983 section a more realistic appearance. Trial calculations using the freshwater content and the Bering Strait inflow given by Östlund & Hut were run, and the expected changes occurred. If their estimate of the freshwater supply is substantiated, it could be worthwhile to examine these changes carefully. However, this implies that the current estimate of the river discharge is off almost by a factor of two, which seems hard to believe.

The values given by Östlund & Hut ultimately derive from the residence time of 10 years in the upper layers obtained from tritium observations, and the assumption that 'vintage year' – the time when the mixing between freshwater and Atlantic water occurs on the shelves – and residence time are equivalent. However, I cannot reconcile a unique 'vintage year' with a horizontally well mixed state, which is implied by the almost universal occurrence of the age of 10 years found in the Polar Ocean. If the tritium age estimate is 5 years too low, the freshwater content would be the same as that used in our work, and the river input and the ice export would both be about $0.1 \cdot 10^9$ kg s^{-1}, which is given by most investigators. In addition, the combined outflow of polar surface water through the Fram Strait and the Arctic Archipelago would be about $2 \cdot 10^9$ kg s^{-1} close to our value.

If a traditional residence time – volume to outflow ratio – is introduced, and the depth

of the upper layer is put to 200 m, we obtain a residence time of 27 years taking our obtained outflows through the Fram Strait and the Arctic Archipelago into account.

It is interesting to note, however, that to exchange this volume in a ten year period would require an outflow of $5 \cdot 10^9$ kg s^{-1}, almost twice the outflow given by Östlund & Hut. This seems to indicate that the residence times of the polar mixed layer and the pycnocline may differ by a factor of 2.

The current measurements discussed by Hanzlick do not quite confirm the large transports given by Aagaard & Greisman (1975). The value $5.6 \cdot 10^9$ kg s^{-1} includes a deep water contribution of $1.9 \cdot 10^9$ kg s^{-1}, and the transport in the upper layers, although large, is only half of the value given by Aagaard & Greisman.

However, it is still about twice the transport obtained here for the West Spitsbergen Current, and since the total transport, not just the baroclinic component is computed, the estimates should agree. We have previously examined the weaknesses in our work, and it is not inconceivable that the transport is off by a factor of 2. Despite this, we shall briefly examine if any sources of error exist which may complicate the interpretation of the direct current measurements.

The main uncertainty results from the fragmentary nature of the West Spitsbergen Current. The current filaments are meandering towards the north. The core passes or bypasses the current meter giving rise to temporal changes of the current. At best the observed time variation and a constant cross section would lead to the same transport estimate as if a current with constant higher velocities, but with smaller spatial extent, were considered. But this is by no means certain. We do not suggest that all time variations are due to a meandering of smaller current filaments, but a substantial part might well be.

Real difficulties would arise if the filaments were quasistationary in space. Then an unfortunate positioning of the instruments might lead to quite erroneous results. In our transport computations (e.g. Fig. 19) we have determined the net transport in each θ–S interval. This was done to eliminate the existence of smaller scale eddies of the size of the Rossby radius (10–20 km). By dividing the section in different parts, the effects of the larger gyres could still be retained. We shall now compute the total transport in each water mass for the different parts to estimate the strength of this eddy field compared to the net transport. As a criterion of this strength we have used the ratio of the sum of the north and south transports to the net transport. We will then also obtain an estimate of how large transports it would theoretically be possible to observe in the West Spitsbergen Current, if the current meters were deployed in the principal inflow areas.

The eddy activity (by our definition) is found to be strongest in the deep water on the eastern side (Fig. 20). Part of this may be real and connected with the motion close to the Molloy Deep, but there may also be some effect of the deep boundary current on the Svalbard slope (stn. 117), which the solution acts to diminish. It should be pointed out that a southward flow in the deeper (and upper) layers in this area has been reported elsewhere (Aagaard et al. 1973; Hunkins 1984).

The eddy activity is also high in the West Spitsbergen Current and in the outflowing modified Atlantic water in the East Greenland Current. This contrasts with the almost uniform outflow found in the western central part, which substantiates our suspicion that the solution tends to displace the outflow towards the deeper, somewhat saltier stations.

In the West Spitsbergen Current the total inflow of deep water is well within the range of what is found from the current measurement, while the inflow of Atlantic water ($2.5 \cdot 10^9$ kg s^{-1}) is still less than the value arrived at by Hanzlick. However, it might be that the balanced solution could produce velocities as large as the mean values found from the current records.

It is not the intention to dismiss the transports implied by the current measurements in

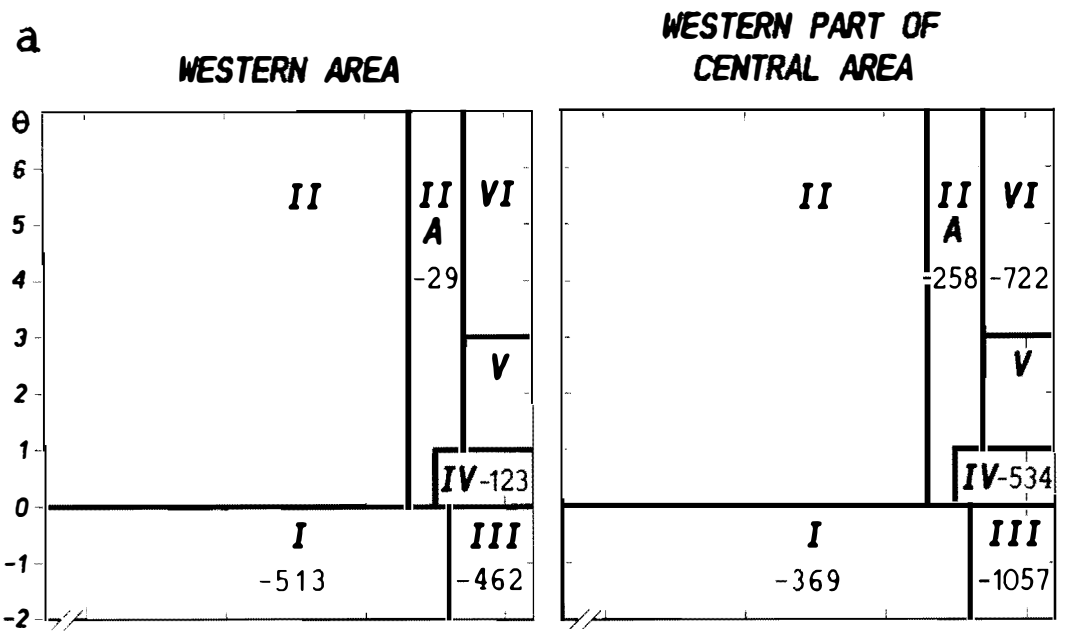

Fig. 19a. Transports of different water masses through parts of the cross section.
Mass and salt continuity required and constraints applied on the deeper layers. Positive flow towards the north.
'Ymer' section.

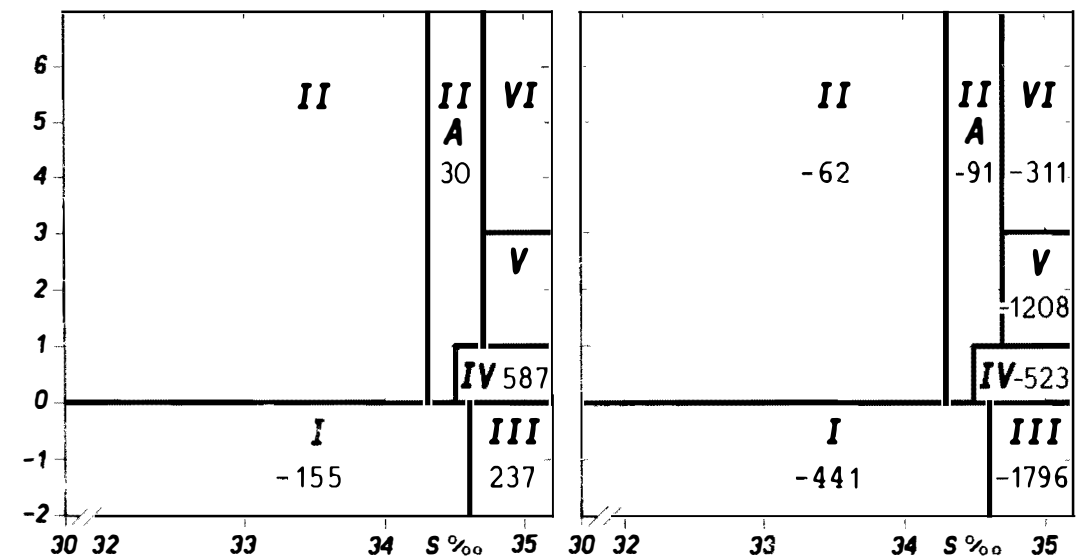

Fig. 19b. Transports of different water masses through parts of the cross section.
Mass and salt continuity required and constraints applied on the deeper layers. Positive flow towards the north.
'Lance' section. kg/s.

a

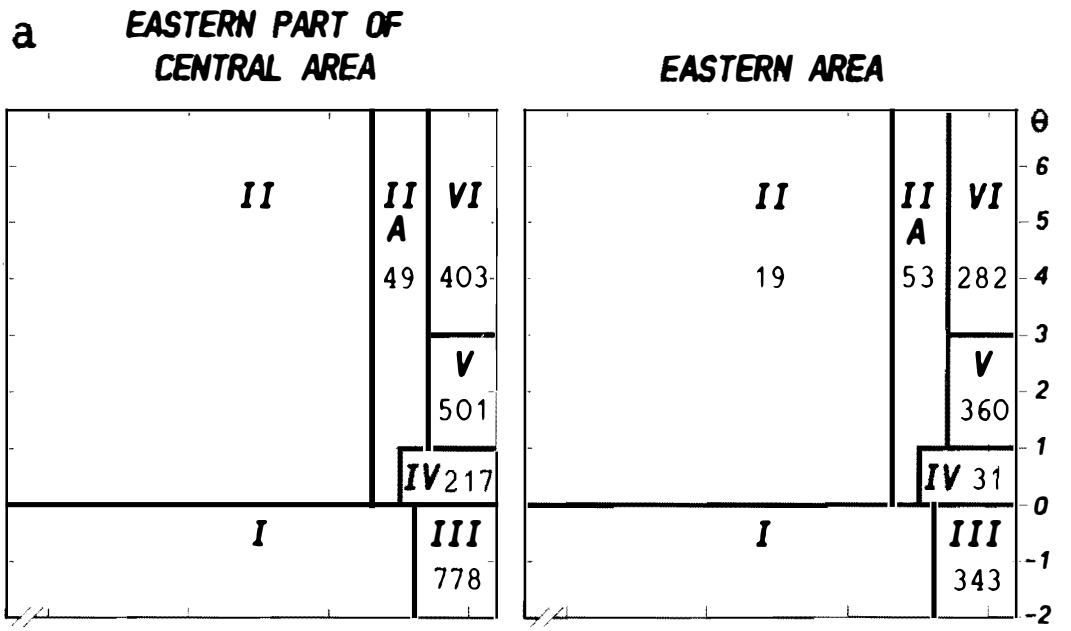
EASTERN PART OF CENTRAL AREA
EASTERN AREA
II
IIA
VI
49
403
V
501
IV 217
I
III
778
II
IIA
VI
19
53
282
V
360
IV 31
I
III
343
θ
6
5
4
3
2
1
0
-1
-2

b

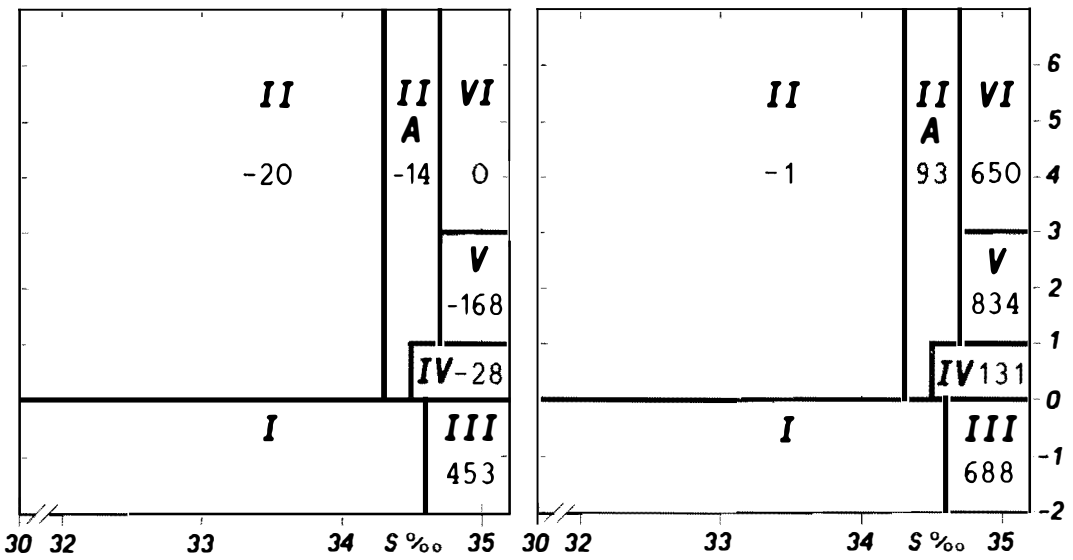
II
IIA
VI
-20
-14
0
V
-168
IV -28
I
III
453
II
IIA
VI
-1
93
650
V
834
IV 131
I
III
688
6
5
4
3
2
1
0
-1
-2
30 32 33 34 S ‰ 35
30 32 33 34 S ‰ 35

Table 3. Transports through the Fram Strait.

	I Mass & Salt balance required		II Mass & Salt balance required constraints on the deep flow	
	10^9 kg/s 'Ymer'	'Lance'	10^9 kg/s 'Ymer'	'Lance'
West Spitsbergen Current				
AW	0.65	−0.09	1.92	1.48
DW	0.58	−1.19	1.12	1.14
East Greenland Current				
PSW	−0.88	−0.54	−0.88	−0.60
AW	−0.50	−0.77	−0.98	−1.61
MAW	−0.36	0.38	−0.69	0.09
Combined total upper circulation	−1.74	−0.93	−2.55	−2.12
DW	0.62	1.09	−1.52	−1.56

Table 4. Exchanges through the Fram Strait ('Ymer' section case II).

	mass transport 10^9 kg/s		heat transport 10^9 kcal/s	
West Spitsbergen Current				
AW	1.9		5.4	
DW	1.1		−1.0	
East Greenland Current				
PSW	−0.9		1.26	
AW	−1.0	−2.6	−1.73	−0.8
MAW	−0.7		−0.34	
DW	−1.5		0.8	
Ice	−0.08		6.4	
Net transport	−1.1		4.4 (excl. ice)	

Table 5. Some transport estimates.

Passage	Mosby 1962 Sv	Aagaard & Greisman 1975 Sv	Stige-brandt 1981 Sv	Fletcher 1965 Sv	Hanzlick 1983 Sv	Östlund & Hut 1984 Sv
The Arctic Archipelago	−1.1	−2.1	−2.0	−1.1		*
The Bering Strait	1.2	−1.5	1.5	1.0		*
The Barents Sea	−0.05	0.6	0	1.0		*
The Fram Strait						
West Spitsbergen C.						
AW	1.4	7.1	2.0	3.2	3.7	2.8*
DW	0.6	0	0		1.9	
East Greenland C.						
PSW	2.0	−1.8	−1.5	4.0		−2.9*
AW			0			
MAW		−5.3	0			
DW		0	0			
Ice	−0.04	−0.1	−0.08	−0.1		−0.15*
Run off	0.12	0.1	0.1	0.14		0.18
Net. precip.	0.01					

* Östlund & Hut do not distinguish between the different in- and outflow. With an inflow of 1.5 Sv through the Bering Strait the Atlantic inflow would be 1.3 Sv and the salinity of the total outflow about 32.45 ‰, which is rather low. Finally their tables 4 and 5 give different values on the ice export. To our mind it should be 0.15 Sv. The net export to the Barents Sea would then be 0.01 Sv close to our estimated ice melt in the southern Barents Sea 0.008 Sv (sect. 5).

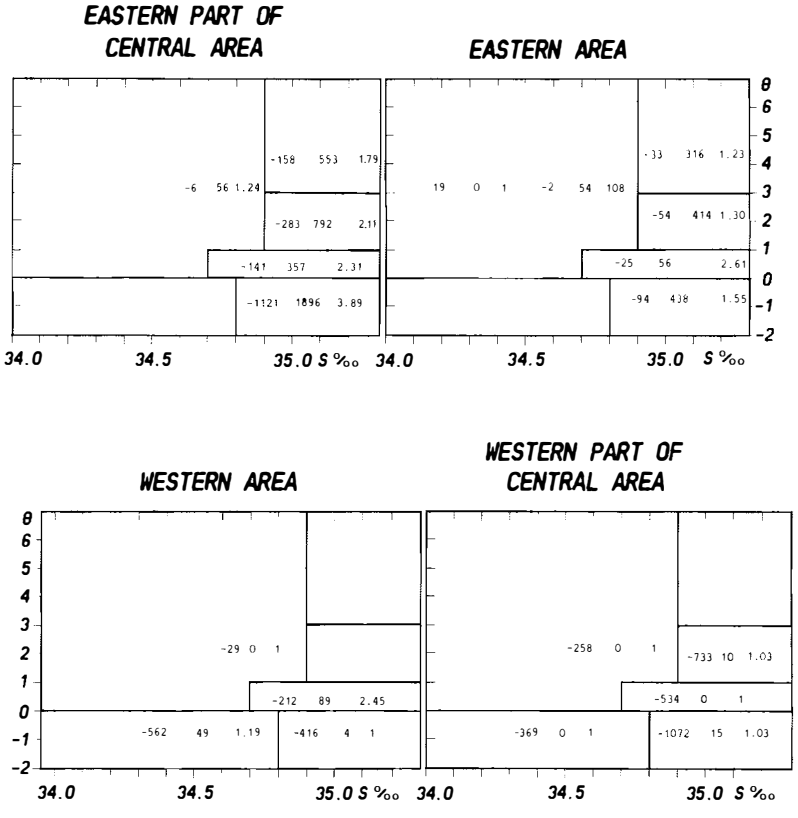

Fig. 20. Total in- and outflow and strength of the eddy field in different parts of the cross section. Mass and salt continuity required and constraints applied on the deeper layers. Positive flow towards the north. 'Ymer' section. kg/s.

such a cavalier fashion, but merely to see if there exists any real contradiction between the different results. The chances of deploying the moorings solely in concentrated inflow areas are remote, and considering the manner in which we have dealt with our unwanted sections, we are hardly in a position to criticize.

In view of the different approaches used in these three works the transport estimates agree surprisingly well. The present results are then in the same range as those found by most investigators. If and when more accurate constraints become available, possibilities exist of improving the estimates.

The main methodological problem still remains. Could a variational approach be expected to adequately describe a system as complex as the flow field in the Fram Strait, and is the choice of variational function the most appropriate? To these questions we have no compelling answers.

9. Discussion

The most significant moral drawn from Table 5 giving the various transport estimates may be the difficulty in making even a slight improvement upon previous figures and short 'back of the envelope calculation'. It is doubtful that any better results will be at hand until some understanding of the different processes which drive the exchanges, especially through the Fram Strait, has been reached.

In the sections above, dealing with the transports through the Bering Strait, the Arctic Archipelago, and the Barents Sea, a more or less accepted dominant driving force was assumed. By contrast, in the work on the Fram Strait, no hypothesis, except the condition of geostrophically balanced flow, was put forth. No explanation for the observed stratification and the position of the resulting level of no motion was given, or needed. We shall therefore conclude this work with a brief review of the different processes which we believe are instrumental in driving the exchanges through the Fram Strait.

The most important single factor in the Polar Ocean–Greenland/Norwegian Seas system is probably the freshwater supply to the Polar Ocean. This is capable of driving an estuarine circulation through the Arctic Archipelago and the Fram Strait (Stigebrandt 1981b). The effect of this positive buoyancy contribution is enhanced by the dense and homogeneous water column found to the south in the Greenland Sea.

The resulting pressure gradients drive a surface flow soutward and a compensating return flow in the deeper layers into the Polar Ocean. The cooling and the formation of ice during the winter, in the Polar Ocean as well as in the Greenland Sea, complicate this picture. In both areas deep water formation occurs, and the newly formed waters leave their respective basins through the Fram Strait, probably as topographically steered boundary currents, the NSDW to the east and the PODW to the west. Some GSDW penetrates north directly into the central parts of the Fram Strait. A deep thermodynamically driven exchange thus takes place in addition to the main one due to the freshwater input.

To conserve mass and salt a return flow is needed to compensate for the outflow of Polar surface water. However, it is not a priori necessary that such an inflow occurs through the Fram Strait. It may just as well take place over the Barents Sea or be supplied from the Pacific through the Bering Strait. What drives an Atlantic inflow through the Fram Strait is thus a question of some importance. From a purely baroclinic point of view one would expect the northward drift of Atlantic water in the Norwegian Sea to turn west to cover the dense surface water in the Greenland Sea gyre. However, a reversal in depth of the pressure gradients between the Greenland Sea and the Polar Ocean and the existence of a meridional boundary could force the Atlantic water north along the western side of the Yermak Plateau.

This inflow is augmented by the presence of light surface water deriving from the Barents Sea on the west coast of Svalbard. This could transform part of the West Spitsbergen Current into a buoyant boundary current akin to the Norwegian coastal current and make it turn east into the Polar Ocean north of Svalbard.

So far the effects of the winds have been neglected. Aagaard (1970) and Hanzlick (1983) have suggested that perhaps the largest contribution to the West Spitsbergen Current is due to the predominantly cyclonic wind field found over the Greenland/Norwegian Seas. This results in a northward Sverdrup transport, which is channelled into the West Spitsbergen Current by the topography (the Mohn Ridge) (Hanzlick 1983; Greisman & Aagaard 1979). While such an effect undoubtedly would be present in our sections, it is not certain that it would prevail further north outside the forcing area when the Atlantic water encounters the polar surface water off the Yermak Plateau. Some local pressure gradient is then necessary to force the Atlantic water further north.

The introduction of the wind effects as a Sverdrup transport is an interesting idea, which perhaps could be applied with equal success to the interior of the Polar Ocean. The predominantly anticyclonic wind field over the Beaufort Sea (Colony & Thorndike 1984) creates an oceanic high over the Beaufort Sea, which incidentally forces the transports through the archipelago. In addition, we would expect a southward Sverdrup transport to exist in the Beaufort Sea driving water towards western Canada, Alaska, and the Chukchi Sea. The wind field is cellular rather than zonal, and no meridional boundary is necessary

to establish the return flow in a 'western' boundary current. The return flow will hang on the western side of the oceanic high, intensify as it approaches the Pole and then start to diverge with the changing sign of the β effect – no problem with separation from the coast. Most of the Trans-Polar-Drift exits through the Fram Strait, where Greenland provides the meridional boundary necessary for currents to cross latitudes. Some part of the Trans-Polar-Drift may also leave through the Robeson-Kennedy Channel.

To estimate the magnitude of such a circulation we use the pressure maps given by Colony & Thorndike (1984). With air pressure gradient of $\Delta P\, \Delta l^{-1}$, $\Delta P \sim 2$ mb, $\Delta l \sim 800$ km the geostrophic wind is estimated to $U \sim 1.4\ m\ s^{-1}$ ($f = 1.44 \cdot 10^{-4}\ s^{-1}$, $\rho = 1.27 \cdot 10^{-3}$ g cm^{-3}). Using $\tau = c\varrho U|U|$ with $c = 1.3 \cdot 10^{-3}$, we obtain $\tau \sim 0.03\ g\ m^{-1}s^{-2}$. Following the qualitative discussions given in Stern (1975 ch. 2 and 7), we may write the total southward transport T as

$$T = \int_0^L T_y\, dx = \beta^{-1} \int_0^L \mathrm{curl}\ \tau\, dx \sim \beta^{-1} \frac{2\tau L}{2\Delta l}$$

and with $\beta(80^0) = 4 \cdot 10^{-14}\ m^{-1}s^{-1}$ and L = 1500 km the transport becomes:

$$T = 1.4 \cdot 10^9\ kg\ s^{-1}$$

These are very approximative figures but should be correct within a factor of 2 or 3. Some of this Sverdrup transport probably exits through the archipelago, while the major part is fed into the Trans-Polar-Drift towards the Pole and the Fram Strait. The drift is highly unstable. As long as it flows towards the Pole the Coriolis parameter increases, and it becomes more intense. However, if it diverges the planetary vorticity ceases to increase, and the current spreads out. To estimate the width, δ and velocity, v of the Trans-Polar-Drift, we use the approach given by Stern (1975 ch. 2).

We then have

$$v = \left(\frac{2\Delta f T}{h}\right)^{1/2}, \quad \delta = \left(\frac{2T}{\Delta f h}\right)^{1/2}$$

where h is the depth of the upper layers and Δf is the change in Coriolis parameter. Since we have no way of estimating the amount of water which is lost from the current on its way towards the Pole, these estimates are bound to be too high. Assuming that the water moves from 75° to 90° N and that the depth of the upper layer is 200 m, we obtain: v = 26 cm s^{-1}, δ ~ 50 km. These figures are slightly ridiculous, and it is doubtful if the unstable nature of the current could explain a velocity one order of magnitude too high (Colony & Thorndike 1984).

While the β effect may influence the Trans-Polar-Drift, it is not likely that it is of major dynamical importance. The main transport towards the Fram Strait must occur as a rather broad zonal drift, geostrophically balanced by the oceanic high in the Beaufort Sea. Still, the existence of a southward Sverdrup transport in the Beaufort Sea might increase the intensity of this drift, since it implies a rather extensive recirculation in the upper layers of the Polar Ocean and a longer residence time than a simple flow from the Siberian shelves towards the Fram Strait would suggest.

Four mechanisms (freshwater discharge, cooling, ice formation, and the wind fields) are therefore the main constituents in any theory of the exchange between the Polar Ocean and the North Atlantic. To mould these features into a coherent whole is the major problem to be addressed in future work on the mass balance and circulation of the Polar Ocean.

Acknowledgements. – The author wants to thank Professor Gösta Walin for constructive criticism, Professor Knut Aagaard for comments on an early draft, and Professor George Veronis for his critical reading of section 7.3.

Thanks are also due to Alfred Evjen for his assistance with the computer work, to Jorunn Myklebust, Kristina Hansson, and Espen Kopperud for their typing and illustration assistance.

Part of this work was done while the author enjoyed a fellowship from the Nordic University Group for Physical Oceanography. Financial support was also given by Svenska Sällskapet för Antropologi och Geografi through the Andrée Foundation.

References

Aagaard, K. 1970: Wind-driven transports in the Greenland and Norwegian Seas. *Deep-Sea Res. 17,* 281–291.

Aagaard, K., Darnall, C. & Greisman, P. 1973: Year-long Measurements in the Greenland-Spitsbergen Passage. *Deep-Sea Res. 20,* 743–746.

Aagaard, K. & Greisman, P. 1975: Towards new mass and heat budgets for the Arctic Ocean. *J. of Geophys. Res. 80,* 3821–3827.

Aagaard, K., Coachman, L. & Carmack, E.C. 1981: On the halocline of the Arctic Ocean. *Deep-Sea Res. 28,* 529–545.

Aagaard, K., Foldvik, A., Gammelsrød, T. & Vinje, T. 1983: One-year records of current and bottom pressure in the strait between Nordaustlandet and Kvitøya, Svalbard, 1980–81. *Polar Research 1 n.s.*, 107–113.

Aagaard, K., Swift, J.H. & Carmack, E.C. 1985: Thermohaline circulation in the Arctic Mediterranean Seas. *J. of Geophys. Res. 90,* 4833–4846.

Bailey, W.D. 1956: On the origin of Baffin Bay deep water. *J. of Fish. Res. Bd. of Canada 13(3),* 303–308.

Bailey, W.D. 1957: Oceanographic features of the Canadian Archipelago. *J. of Fish. Res. Bd. of Canada 14,* 731–769.

Blindheim, J. & Loeng, H. 1981: On the variability of Atlantic influence in the Barents and Norwegian seas. *Fisk.dir. skr. Havsunders. 17,* 161–189.

Bunker, A.F. & Worthington, L.V. 1977: Energy exchange charts of the North Atlantic Ocean. *Bull. Amer. Meteor. Soc. 57,* 670–678.

Carmack, E.C. & Aagaard, K. 1973: On the deepwater of the Greenland Sea. *Deep-Sea Res. 20,* 687–715.

Claerbout, J. 1976: *Fundamentals of the geophysical data processing.* McGraw-Hill, New York. 274 pp.

Coachman, L.K. & Barnes, C.A. 1961: The contribution of Bering Sea water to the Arctic Ocean. *Arctic 14,* 146–161.

Coachman, L.K. & Barnes, C.A. 1962: Surface water in the Eurasian Basin of the Arctic Ocean. *Arctic 15,* 215–277.

Coachman, L.K. & Barnes, C.A. 1963: The movement of Atlantic water in the Arctic ocean. *Arctic 16,* 8–16.

Coachman, L. & Aagaard, K. 1974: Physical oceanography of the arctic and subarctic seas. Pp. 1–72 in Herman, Y. (ed.): *Marine geology and oceanography of the arctic seas.* Springer Verlag, New York.

Coachman, L., Aagaard, K. & Tripp, R. 1975: *Bering Strait: The regional physical oceanography.* University of Washington Press, Seattle. 172 pp.

Coachman, L. & Aagaard, K. 1981: Reevalution of water transports in the vicinity of Bering Strait. Pp. 95–110 in Hood, D.W. & Calder, J.A. (eds.): *The Eastern Bering Sea Shelf. Oceanography and Resources 1.* Dep. of Commerce/Natl. Oceanic & Atmospheric Admin., Washington D.C.

Collin, A.E. & Dunbar, M.J. 1963: Physical oceanography in Arctic Canada. Pp. 45–77 in Barnes, H.E. (ed.): *Oceanography and Biology, Annual Review 2.*

Defant, A. 1961: *Physical Oceanography 2.* Pergamon Press, London.

Dickson, R.R. & Blindheim, J. 1984: On the abnormal hydrographic conditions in the European Arctic during the 1970s. *Rapp. P. v. Reun. Cons. int. Explor. Mer. 185.*

Fiadeiro, M.E. & Veronis, G. 1982: On the determination of absolute velocities in the ocean. *J. of Marine Research 40,* (suppl.), 159–182.

Fletcher, J.O. 1965: The heat budget of the Arctic Basin and its relation to climate. *The Rand Corporation R. 444-PR.* Santa Monica, California. 179 pp.

Fomin, L.M. 1964: *The dynamic method in oceanography.* Elsevier Publishing Company, Amsterdam. 212 pp.

Greisman, P. & Aagaard, K. 1979: Seasonal variability of the West Spitsbergen Current. *Ocean Modelling 19,* 3–5.

Hanzlick, D.J. 1983: *The West Spitsbergen Current: Transport. Forcing and Variability.* Ph.D. thesis, University of Washington. 127 pp.

Hunkins, K. 1984: Ocean currents and temperatures in the center of Fram Strait during MIZEX 1983. *MIZEX Bulletin IV,* 47–52.

Kiilerich, A.B. 1939: The 'Godthaab' expedition 1928: A theoretical treatment of the hydrographical observational material. *Meddelelser om Grønland 78 (5),* 1–148.

Midttun, L. 1985: Formation of dense bottom water in

the Barents Sea. *Deep-Sea Res. 32(10)*, 1233–1241.

Mosby, H. 1938: Svalbard Waters. *Geofys. Publ. 12(4)*. 85 pp.

Mosby, H. 1962: Water, mass and heat balance of the North Polar Sea and of the Norwegian Sea. *Geofys. Publ. 24(11), 289–313.*

Muench, R. 1971: The physical oceanography of the northern Baffin Bay region. *The Baffin Bay – North Water project. Scientific report No. 1.* Arctic Institute of North America. 150 pp.

Nansen, F. 1906: Northern Waters. Captain Roald Amundsen's oceanographic observations in the arctic seas in 1901. *Vid.-selskap Skrifter I, Mat-Naturv. kl.* Dybwad Christiania 1(3). 145 pp.

Perkin, R.G. & Lewis, E.L. 1984: Mixing in the West Spitsbergen Current. *J. of Phys. Oceanogr. 14,* 1315–1325.

Pfirman, S. 1984: *Water Mass Distributions in the Northern Barents Sea: Summer 1981.* Ph.D. thesis, Woods Hole Oceanographic Institute.

Roemmich, D. 1980: Estimation of meridional heat flux in the North Atlantic by inverse methods. *J. of Phys. Oceanogr. 10,* 1972–1983.

Rudels, B. 1986a: The outflow of Polar Water through the Arctic Archipelago and the oceanographic conditions in Baffin Bay. *Polar Res. 4 n.s.* (in press).

Rudels, B. 1986b: The θ–S structures in the northern seas and their implications for the deep circulation found in the deeper layers of the Polar Ocean and the Greenland/Norwegian Seas. *Polar Res. 4 n.s.* (in press).

Rudels, B. & Andersson, L. 1982: Observations of the mass, heat and salt exchange through Fram Strait. *Report No. 42, Dept. of Oceanography, University of Gothenburg, Sweden.* 17 pp.

Sadler, H.E. 1976: Water, heat and salt transport through Nares Strait, Ellesmere Island. *J. Fish. Res. Bd. of Canada 33(10),* 2286–2295.

SCOR-Working Group 58 1979: The arctic heat budget. *Report No. 52, Geophysical institute, University of Bergen, Norway.* 98 pp.

Schumacher, J.D., Aagaard, K., Pease, C.H. & Tripp, R.B. 1983: Effects of a Shelf Polynya on Flow and Water Properties in the Northern Bering Sea. *J. of Geophys. Res. 88,* 2723–2732.

Smith, E.H., Soule, F.M. & Mosby, O. 1937: The 'Marion' expedition to Davis Strait and Baffin Bay: part II. *Physical oceanography, United States Coast Guard Bull.* 259 pp.

Stern, M.E. 1975: *Ocean circulation physics.* Academic Press, New York. 246 pp.

Stigebrandt, A. 1981a: Is the magnitude of the salinity difference between the North Atlantic and the North Pacific controlled by the topography of the Bering Strait? *Report No. 39, Dept. of Oceanography, University of Gothenburg, Sweden.* 9 pp.

Stigebrandt, A. 1981b: A model for the thickness and salinity of the upper layer of the Arctic Ocean and the relationship between the ice thickness and some external parameters. *J. of Phys. Oceanogr. 11,* 1407–1422.

Stigebrandt, A. 1984: The North Pacific: A global-Scale estuary. *J. Phys. Oceanogr. 14,* 460–470.

Stommel, H. & Veronis, G. 1981: Variational inverse method for study of ocean circulation. *Deep-Sea Res. 28,* 1147–1160.

Swift, J.H. & Aagaard, K. 1981: Seasonal transitions and water mass formation in the Iceland and Greenland seas. *Deep-Sea Res. 28,* 1107–1129.

Swift, J.H., Takahashi, T. & Livingston, H.D. 1983: The contribution of the Greenland and Barents seas to the deep water of the Arctic Ocean. *J. of Geophys. Res. 88,* 5981–5986.

Tancjura, A.I. 1959: On the Currents in the Barents Sea. Trudy. *PINRO 11,* 35–53.

Tchernia, P. 1979: *Descriptive regional oceanography.* Pergamon Press, Oxford. 253 pp.

Vinje, T. 1982: The drift pattern of sea ice in the Arctic with particular reference to the Atlantic approach. In Rey, L. (ed.): *The Arctic Ocean: the hydrographic environment and the fate of pollutants.* MacMillan Press.

Vinje, T. 1983: On the present state and the future fate of the Arctic sea ice cover. Pp. 39–57 in s'Jacob, H.K., Snoeijing, K. & Vaughan, R. (eds.): *Arctic whaling: Proceedings of the intern. symp. Arctic whaling Febr. 1983.* Arctic Centre, Univ. of Groningen, Netherlands.

Vinje, T. & Finnekåsa, Ø. 1986: The ice transport through the Fram Strait. *Norsk Polarinstitutt Skrifter 186.*

Vowinckel, E. & Orvig, S. 1970: The climate of the North Polar Basin. In Orvig, S. (ed.): *World climate survey, Vol. 14: Climates of the polar regions.* Elsevier Publishing Company. 370 pp.

Wunsch, C. 1978: The North Atlantic general circulation west of 50° W determined by inverse methods. *Rev. of Geophys. and Space Phys. 11,* 583–620.

Wunsch, C. & Grant, B. 1982: Towards the general circulation of the North Atlantic. *Progr. in Oceanogr. 11,* 1–59.

Zubov, N.N. 1945: *Arctic Ice.* (Translated from Russian 1965. U.S.N. Oceanographic Office and American Meteorological Society.)

Östlund, H.G. & Hut, G. 1984: Arctic Ocean Water Mass Balance from Isotope Data. *J. of Geophys. Res. 89,* 6373–6381.